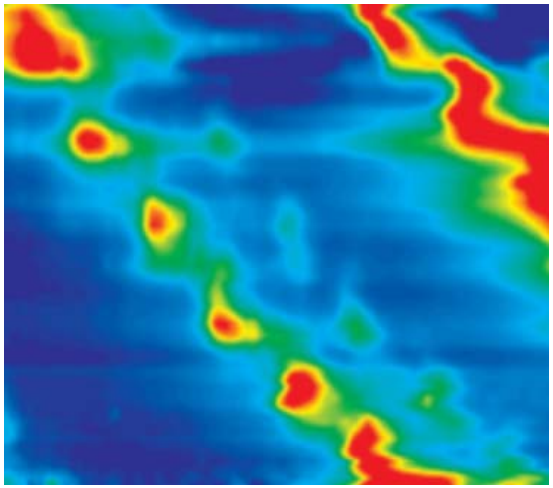

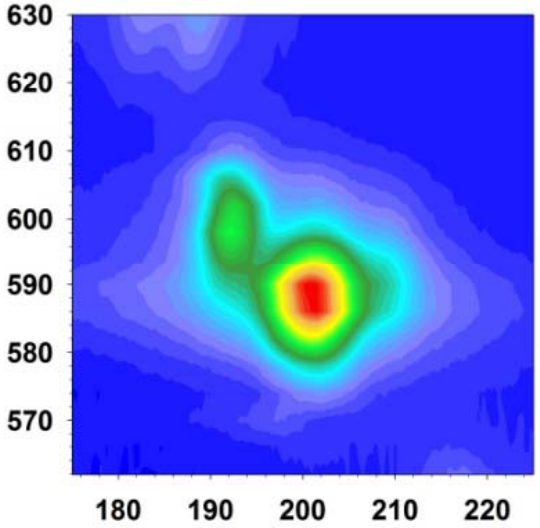

Resonance Raman Studies of Exciton Behavior In Single-Walled Carbon Nanotubes

Stephen K. Doorn
Los Alamos National Laboratory

NNSA

Los Alamos

Presentation Overview

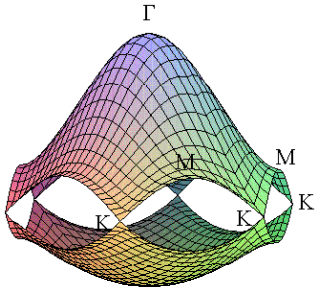

1. SWNT Background

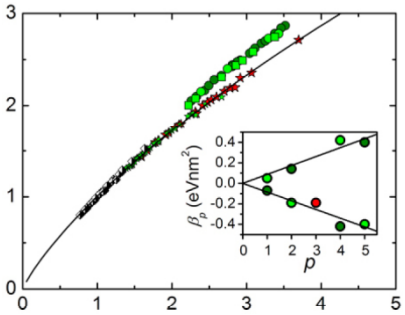

2. Excitonic Behavior of Semiconducting Nanotubes

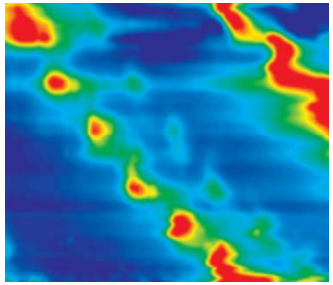

3. Electronic Behavior of Metallic Nanotubes

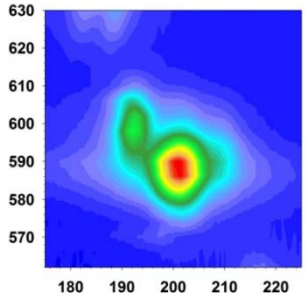

4. Raman of Enriched Metallic Samples

NNSA

Los Alamos

LANL Nanotube Effort

Fundamental Spectroscopy

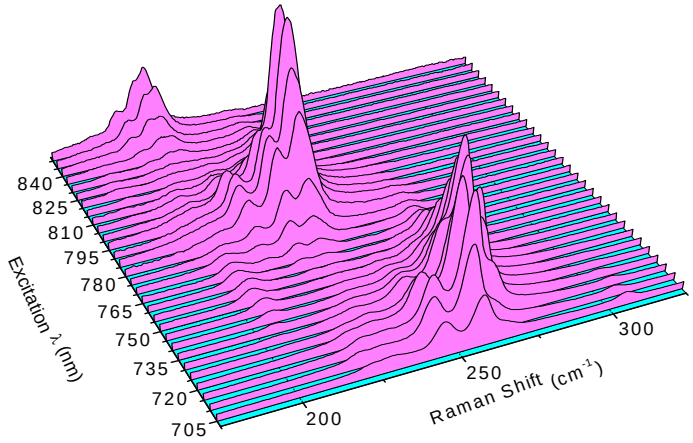

Nanotube Redox Chemistry

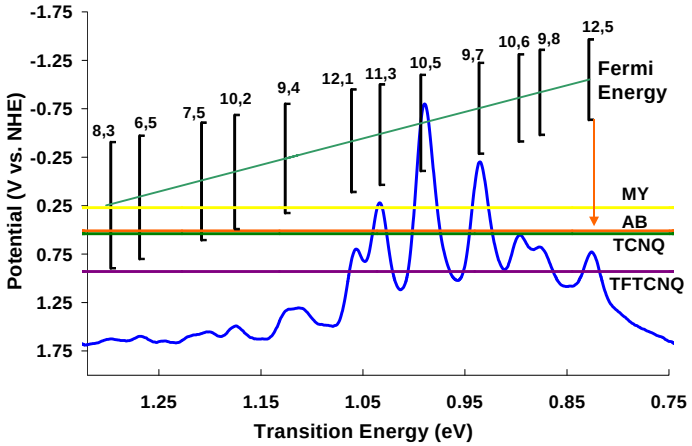

Nanotube Separations

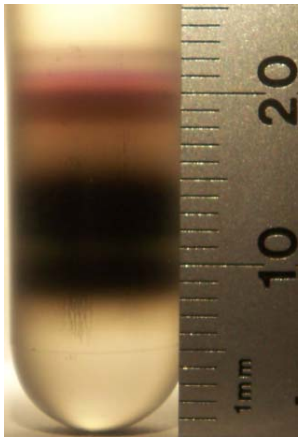

Nanotube-Based Sensing

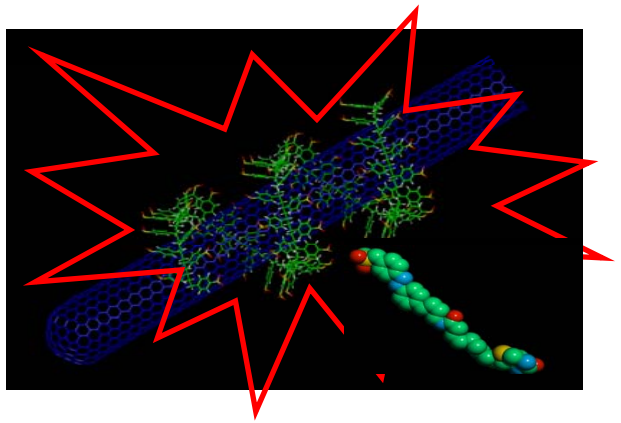

NASA

Los Alamos

Example Applications

Nanoscale Electronics

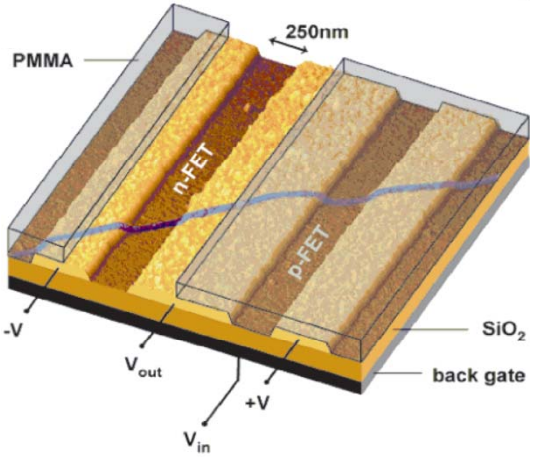

Derycke, et. al., *Nano Lett.* **1**, 453 (2001).

Opto-Electronics

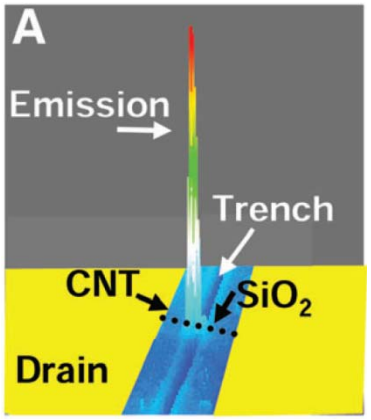

Chen, et. al., *Science.* **310**, 1171 (2005).

Optical Biosensing

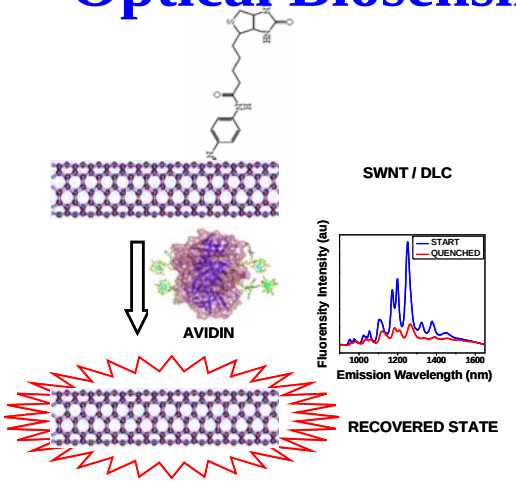

Satishkumar, et. al., *Nature Nanotech.* **2**, 560 (2007).

Fundamental Issues:

--what is the electronic structure?

--what is the nature of the optically excited state?

--how do electrons/excitons couple to phonon structure?

NNSA

Los Alamos

Construction of Nanotubes from a Graphene Sheet

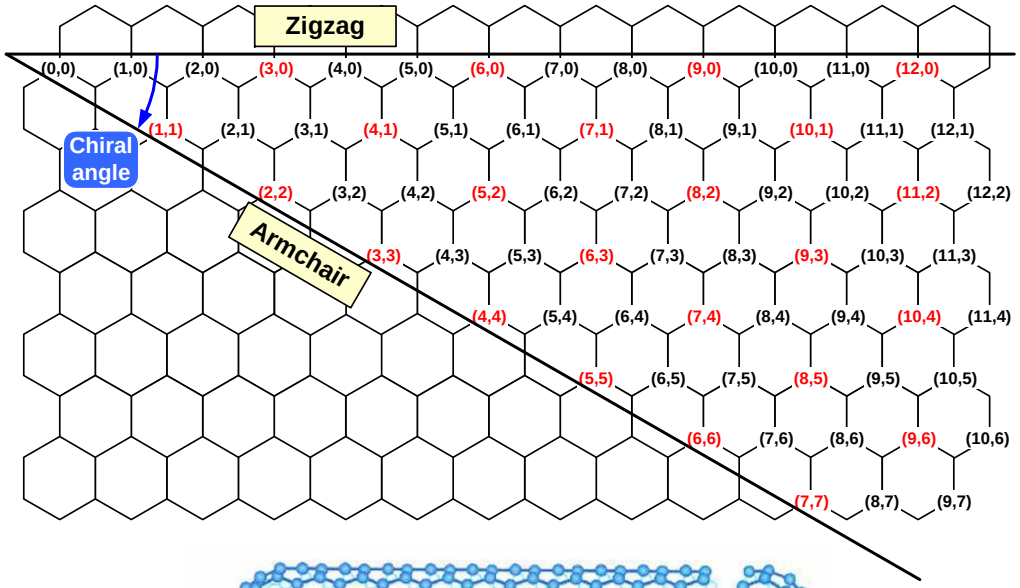

Roll-up Indices (n,m)
Reveal Structural and
Electronic Character

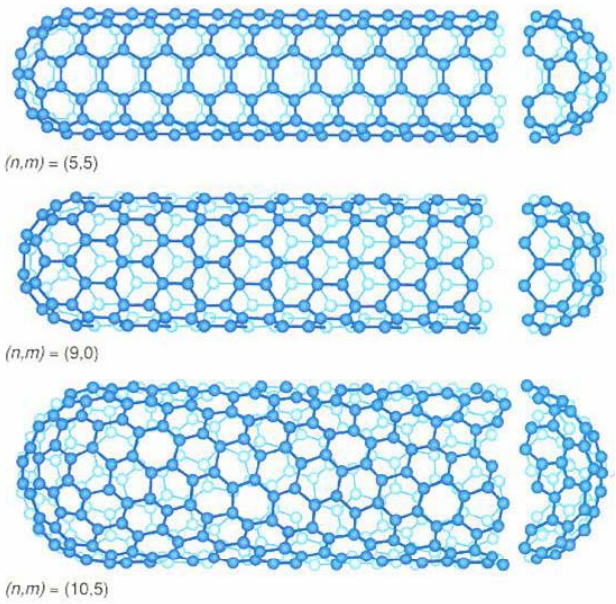

(n-m,mod3) = 0 metallic

(n-m,mod3) = 1

(n-m,mod3) = 2

} semiconductor

Nature of Electronic Excited States

Band Model *vs.* Excitonic Description

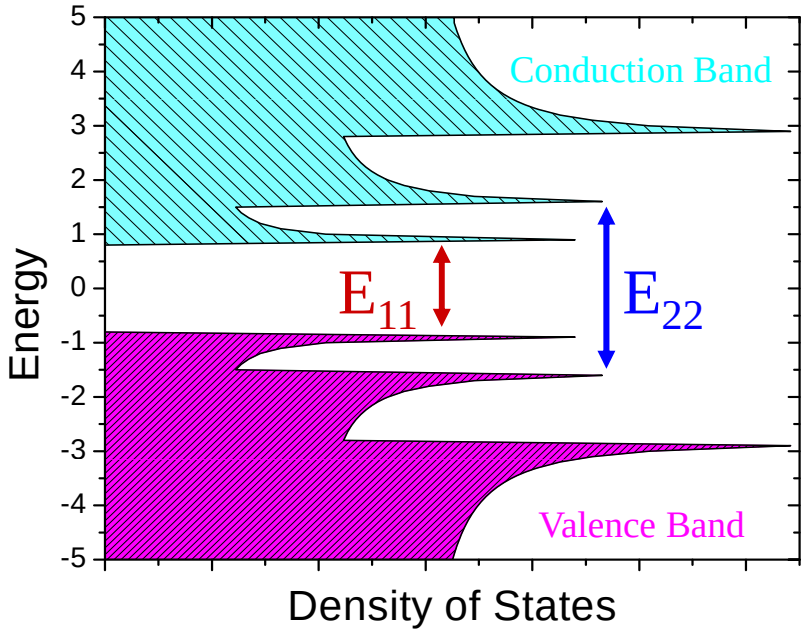

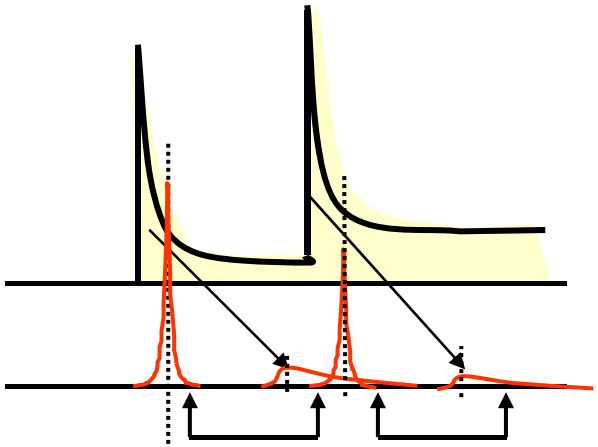

T. Ando J. Phys. Soc Japan
66, 1066 (1997)

Experimental Deviation from Tight-Binding Description

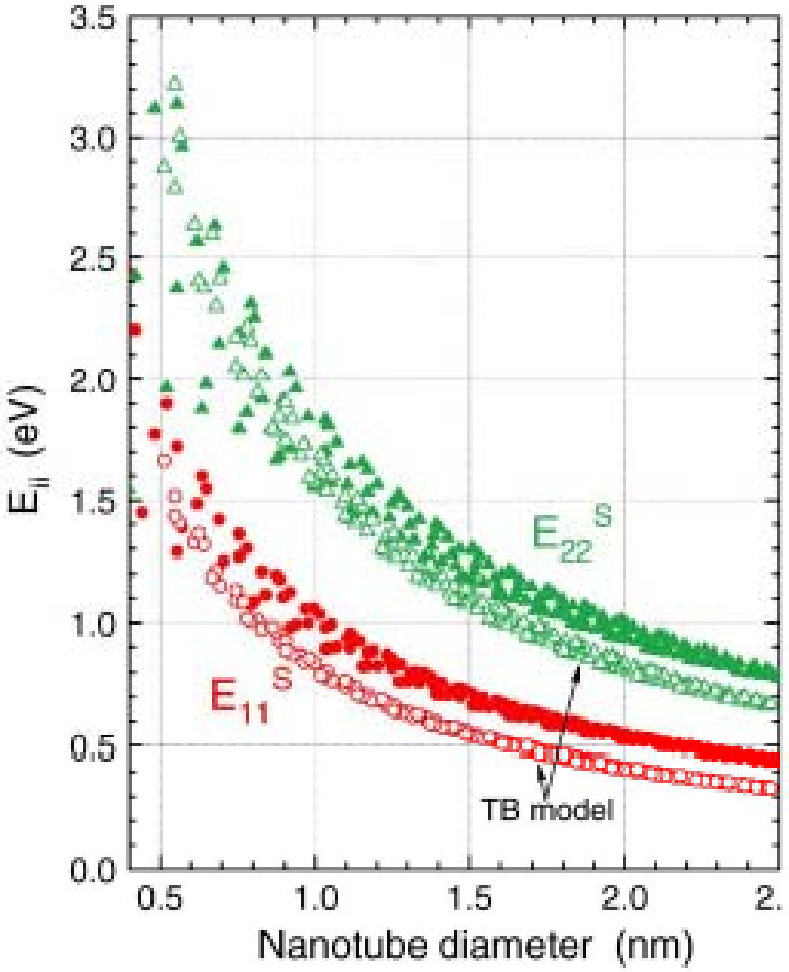

R.B. Weisman, S.M. Bachilo, D.Tsyboulski, *Appl. Phys. A*, **78**, 1111 (2004).

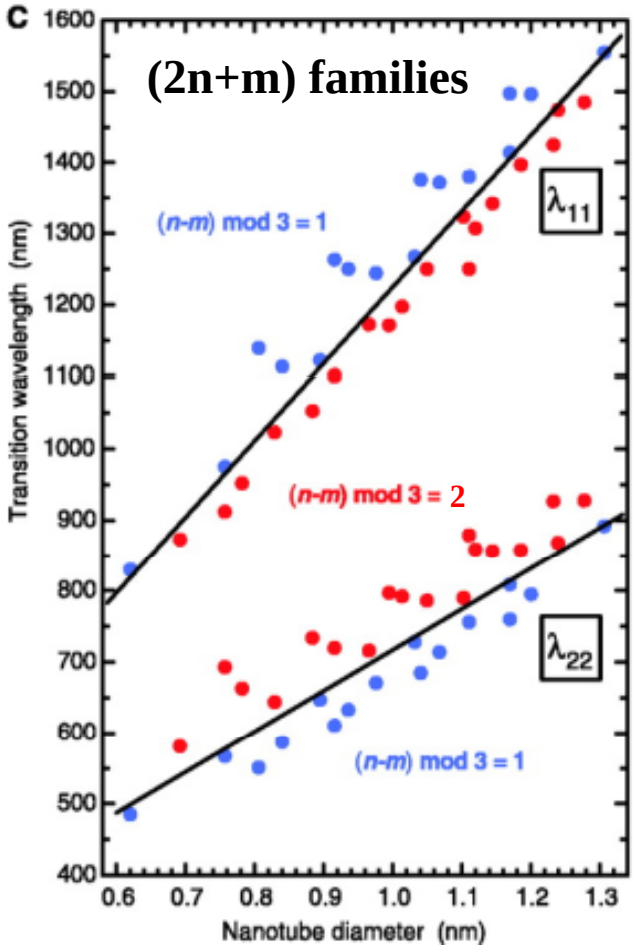

S.M. Bachilo et. al., *Science*, **298**, 2361 (2002).

NASA

Los Alamos

Raman Spectroscopy Is….

Vibrational:

$$\omega_{RBM} = \frac{C_1}{d_{SWNT}} + C_2$$

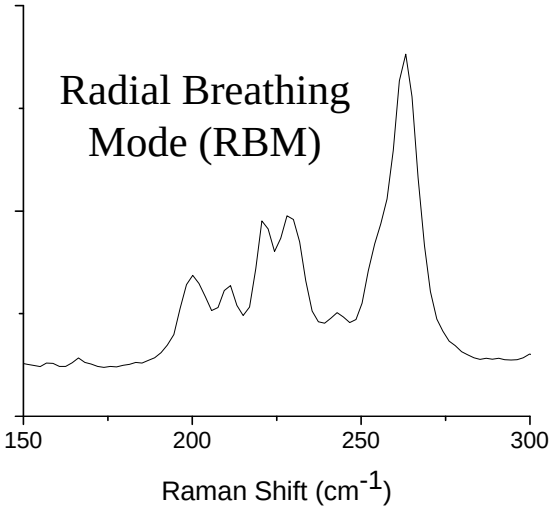

Electronic:

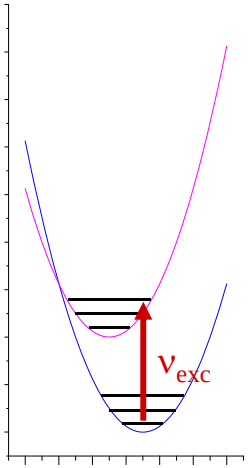

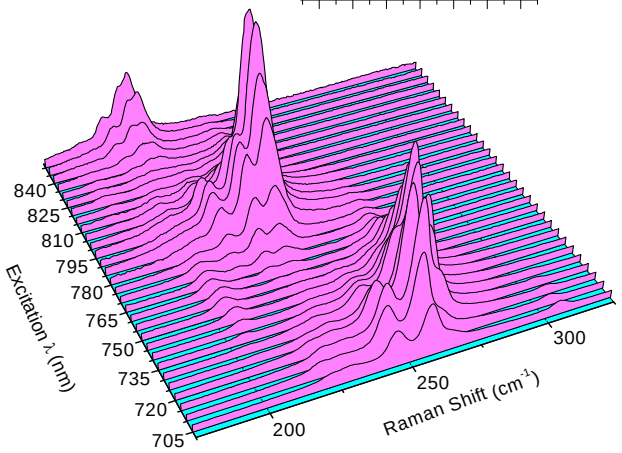

Imaging:

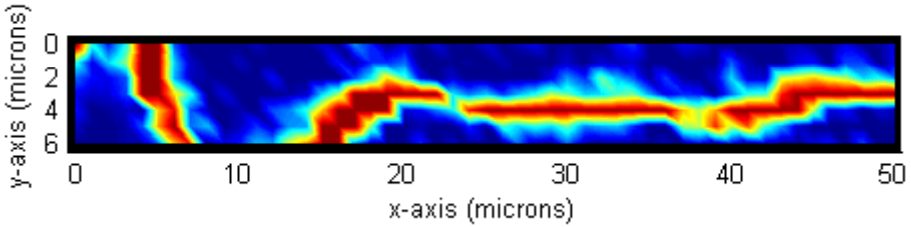

NNSA

Los Alamos

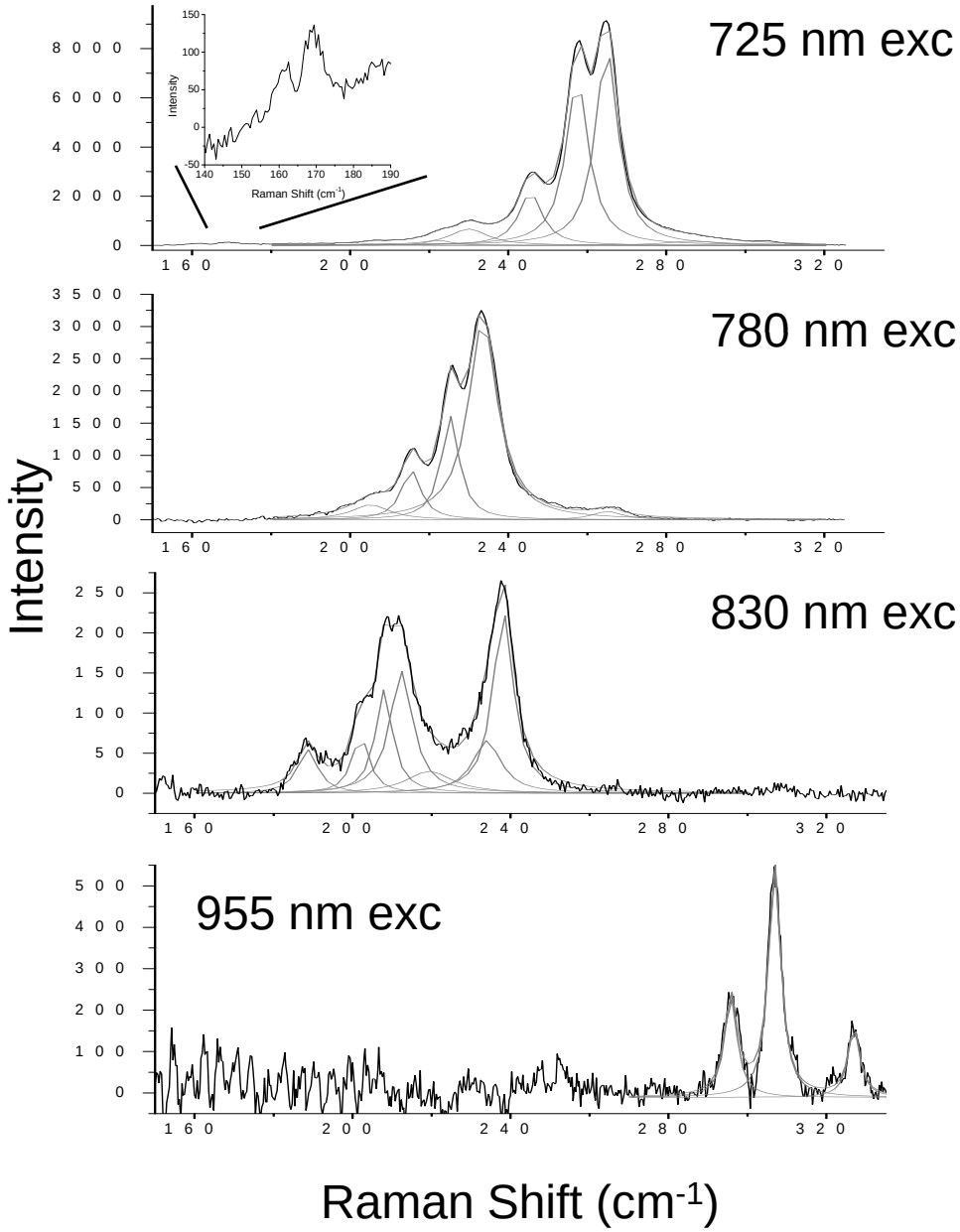

Raman on SDS Solubilized HiPco NTs

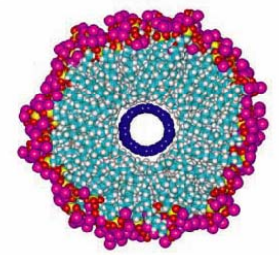

Individualized HiPco nanotubes with observed diameters ranging from 0.6 to 1.6 nm.

Variation in $E_{v.H.}$ with chirality results in sampling of different chiral groupings as Raman excitation is tuned.

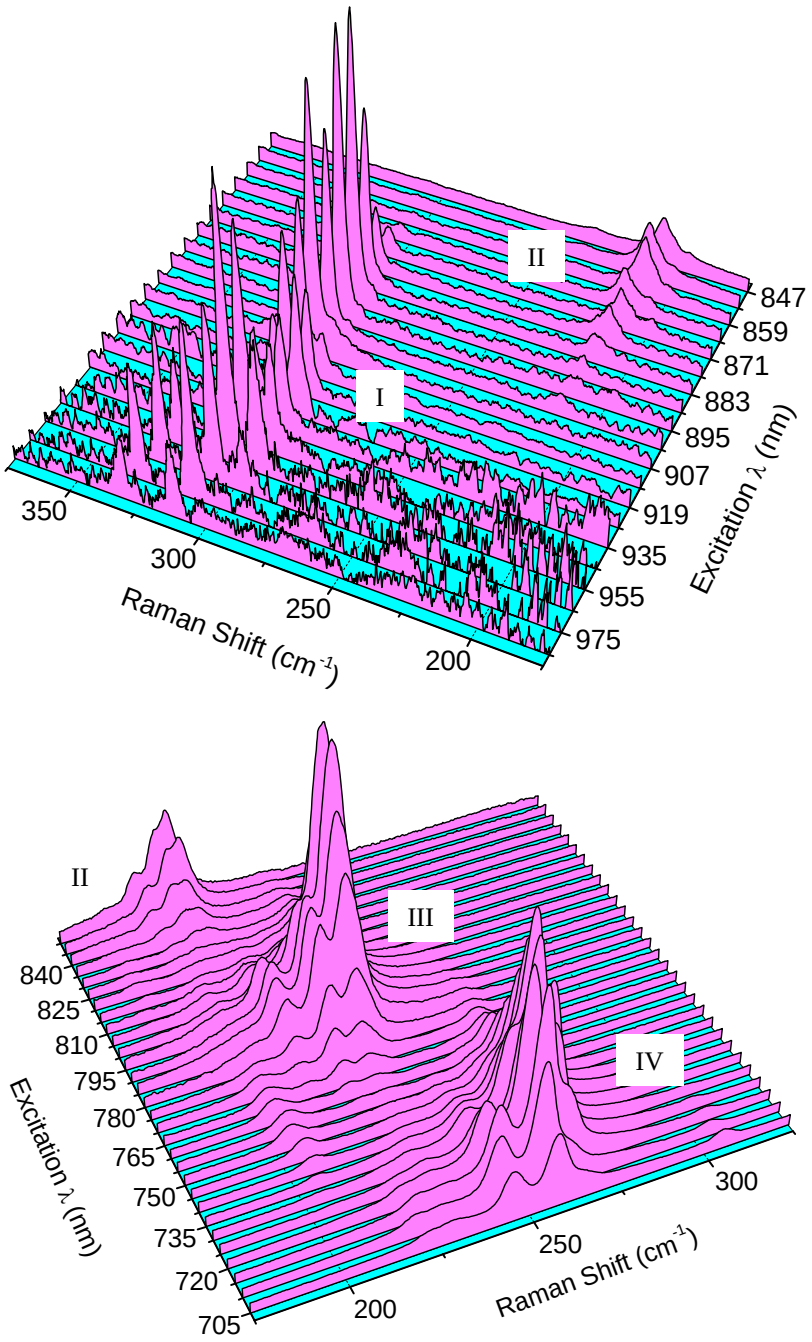

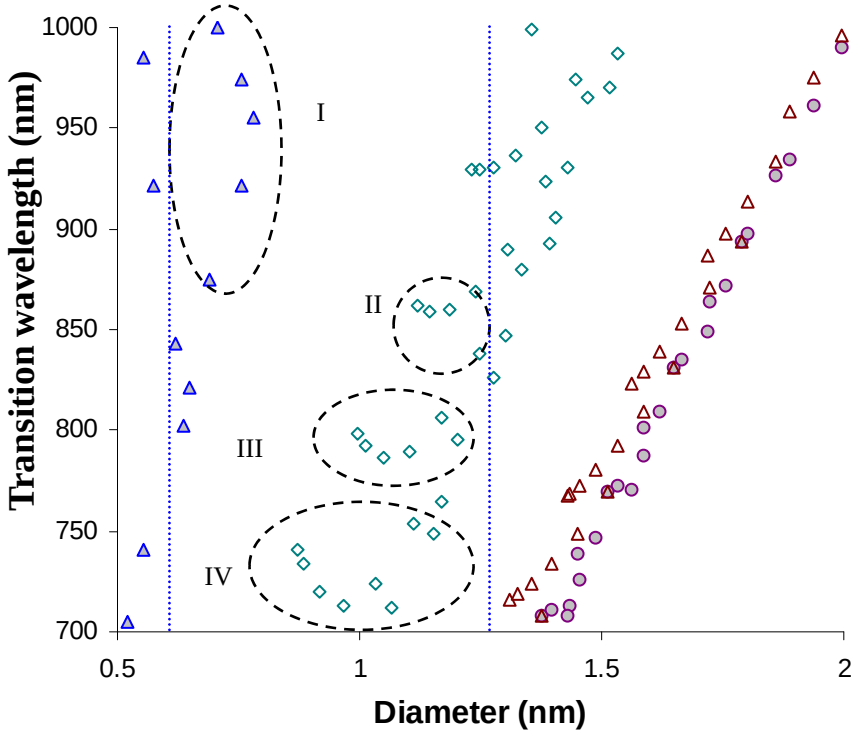

S.K. Doorn, et. al., *Appl. Phys. A*, **78**, 1147 (2004).

NASA

Los Alamos

Chirality Dependence of Raman Scattering Intensity

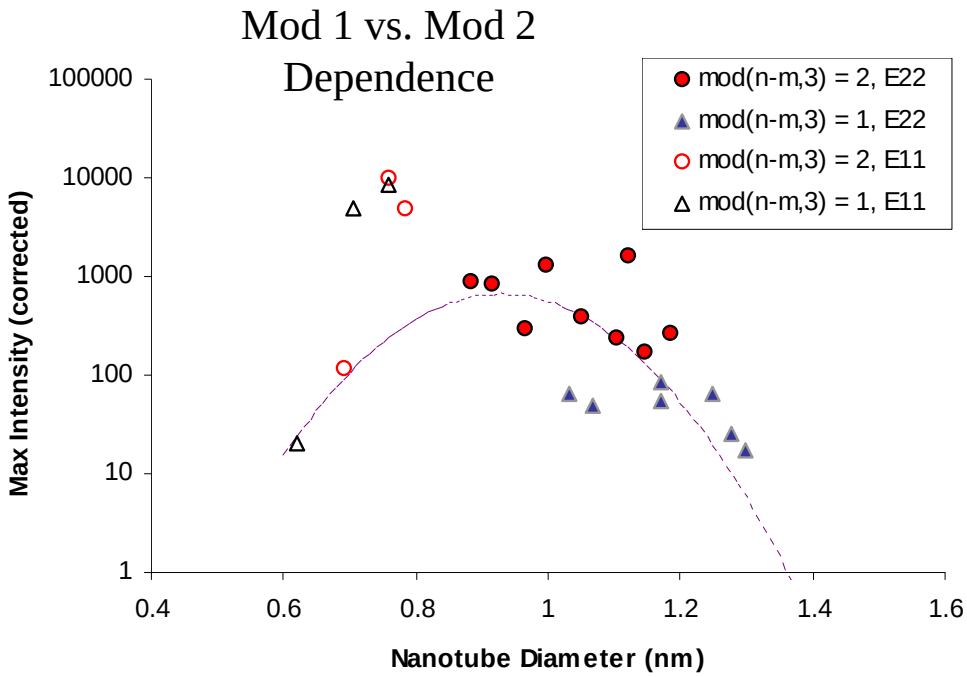

S.K. Doorn, et. al., *Appl. Phys. A*, **78**, 1147 (2004).

Chiral dependence reverses on going from E_{11} to E_{22} excitation.

Explains weakness of (6,4) and (8,4) chiralities with E_{11} excitation. Are strong with E_{22}.

$$\alpha = \sum_{i,j} \frac{M_{ee}^{g,i} M_{ee}^{i,g} M_{ep}^{i,j}}{(E_{laser} - E - i\Gamma_r)(E_S - E - i\Gamma_r)}$$

NASA

Los Alamos

Originates in exciton-phonon coupling.

$$\hat{V}^{\mathrm{RBM}}_{\mathrm{exc-ph}} \propto \left[\frac{\partial\gamma_0(\tau_l)}{\partial\tau_l} - 3\,\delta_0(\tau_l)\,\frac{\partial\sigma_0(\tau_l)}{\partial\tau_l}\right] \mathbf{X}$$

$$\left\{sign(n_e+\nu/3)\,\cos 3\theta + \frac{5}{4\sqrt{3}}\,\frac{a}{R}\,|n_e+\nu/3|\left(1+\frac{\cos^2 3\theta}{5}\right)\right\}$$

S.V. Goupalov, *Phys. Rev. B*, **71**, 153404 (2005).

S.V. Goupalov, B.C. Satishkumar, S.K. Doorn, *Phys. Rev.B*, **73**, 115401 (2006).

Chiral Angle Dependence

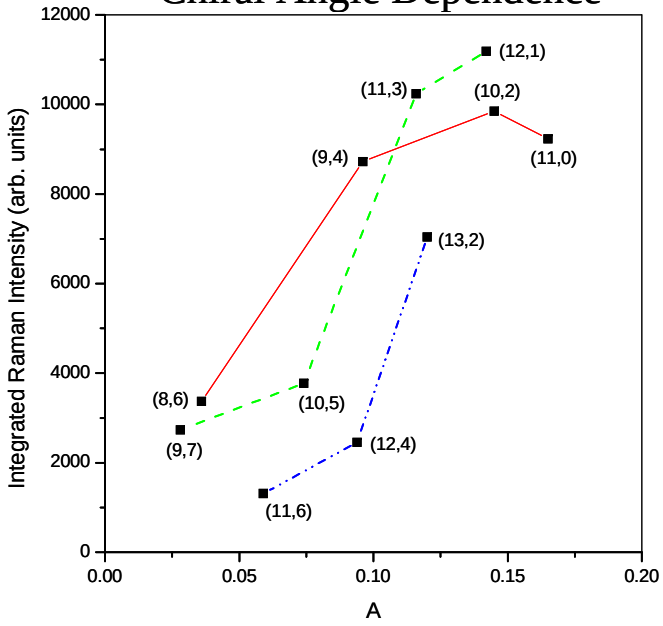

Phonon Scattering And Transport

V. Perebeinos, et.al. *Phys. Rev. Lett.*, **94**, 086802 (2005)

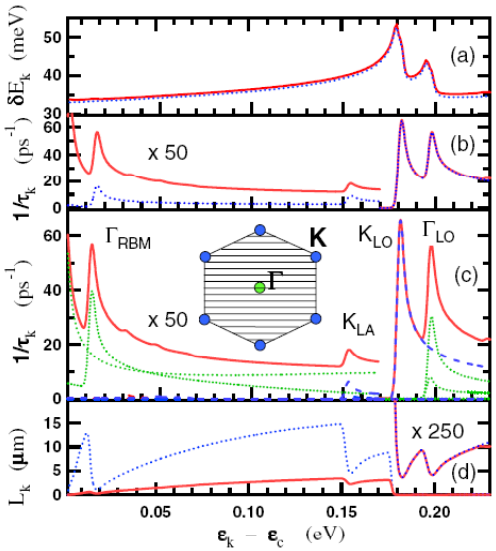

Electronic Structure at High Excitation Energies

E_{11} and E_{22} Excitations Produce Bound Excitons
What About E_{33} and E_{44}?

Raman on
Vertical Arrays

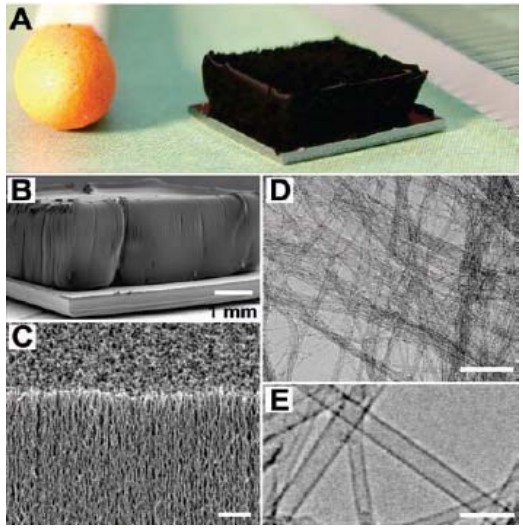

K. Hata et al. Science 306, 1362 (2004)
Murakami et. al. Carbon, 43 2664 (2005)

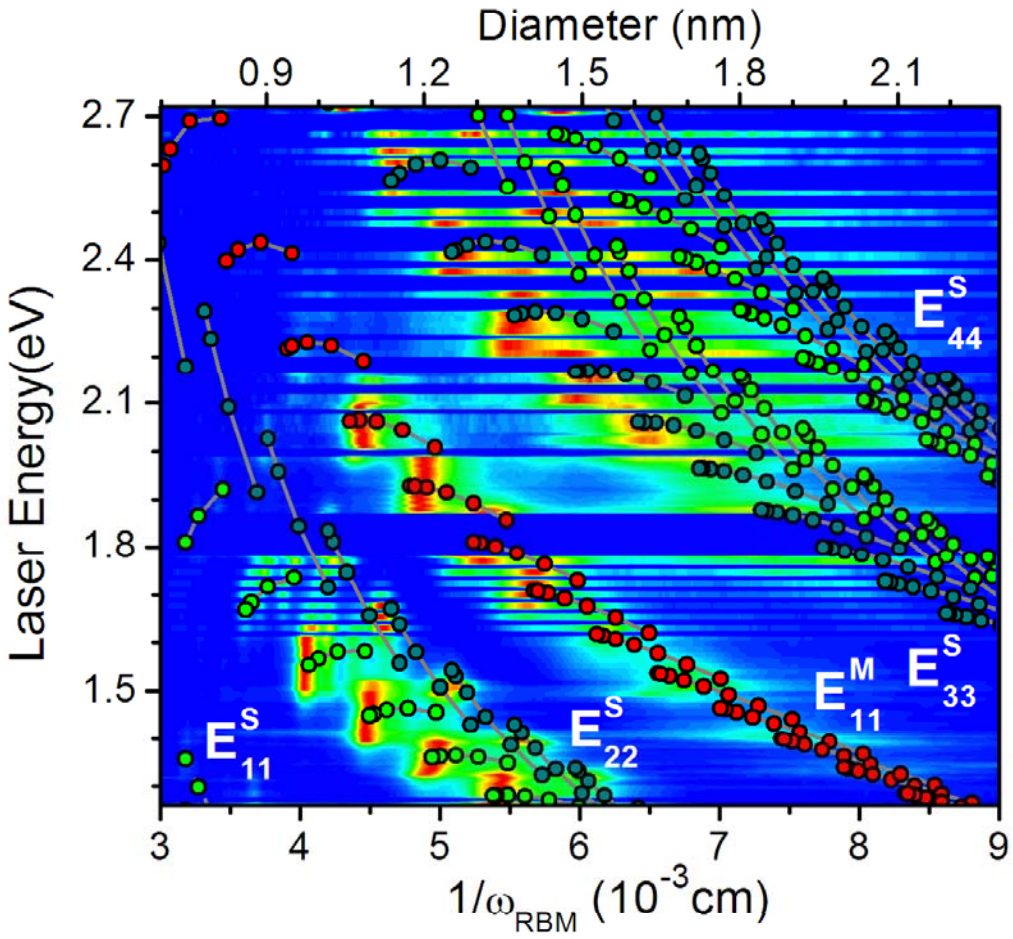

NASA

Los Alamos

E33/E44 Energy Behavior Departs From E11/E22

P.T. Araujo, et. al., *Phys. Rev. Lett.* **98**, 067401 (2007).

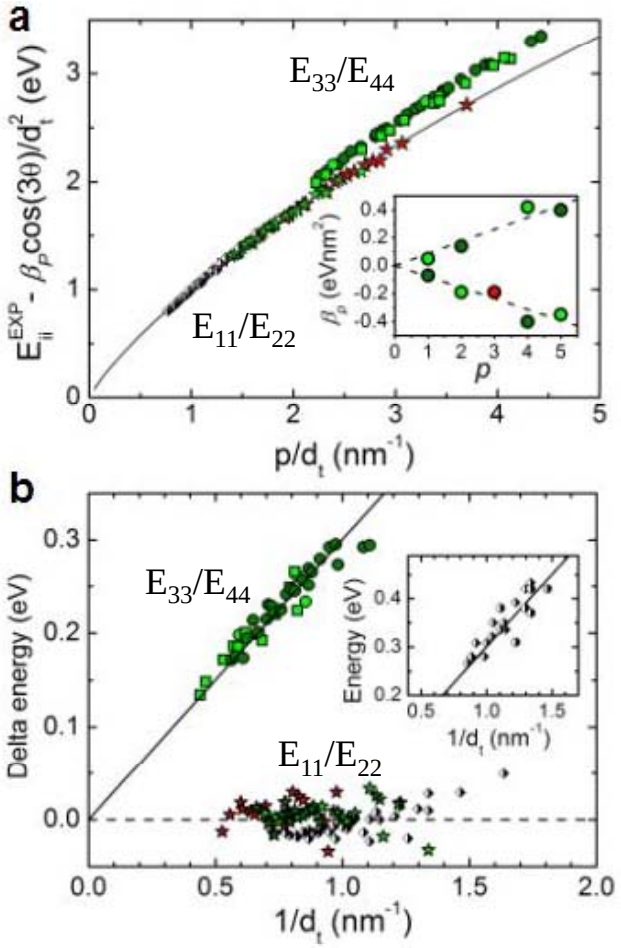

Nonlinear Scaling Analysis
Of Transition Energies

$$E_{ii}(p,d_t) - \beta_p \cos 3\theta/d_t^2 = a\,\frac{p}{d_t}\left[1 + b \log \frac{c}{p/d_t}\right]$$

Chirality dependence — Single Particle Energy — Coulomb Contribution

For E_{33}, E_{44}:

Add Additional factor of $0.305/d_t$

Implicates change in excitonic behavior.

NASA

Los Alamos

Reflection of Decrease In Binding Energy?

-OR-

Reflection of Assymetric Increase In Self-Energy?

Quantum chemistry calculation shows delocalized electron wavefunction

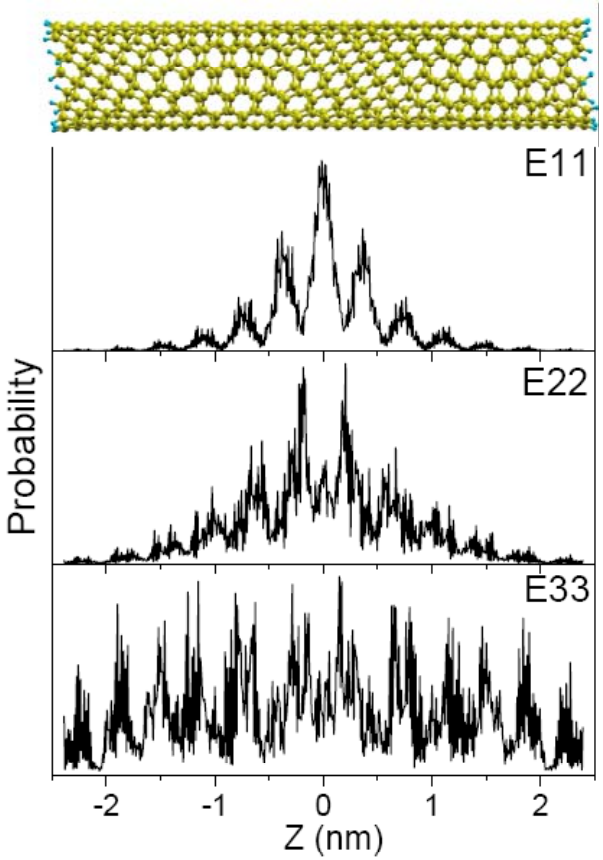

*P. T. Araujo et al. PRL **98**, 067401 (2007)*

Self-energy increases faster than binding energy.

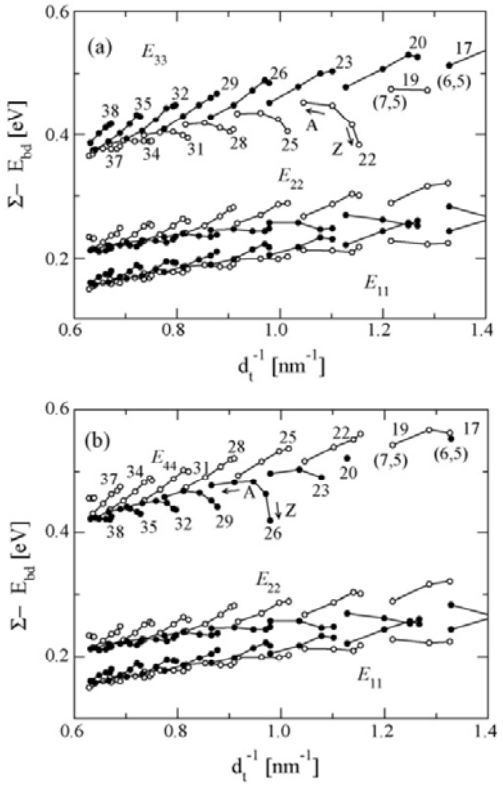

*K. Sato et al. Vib. Spect. **45**, 89 (2007)*

NASA

Los Alamos

Curvature Effects on E33 and E44 Exciton Energies

RBM Spectra

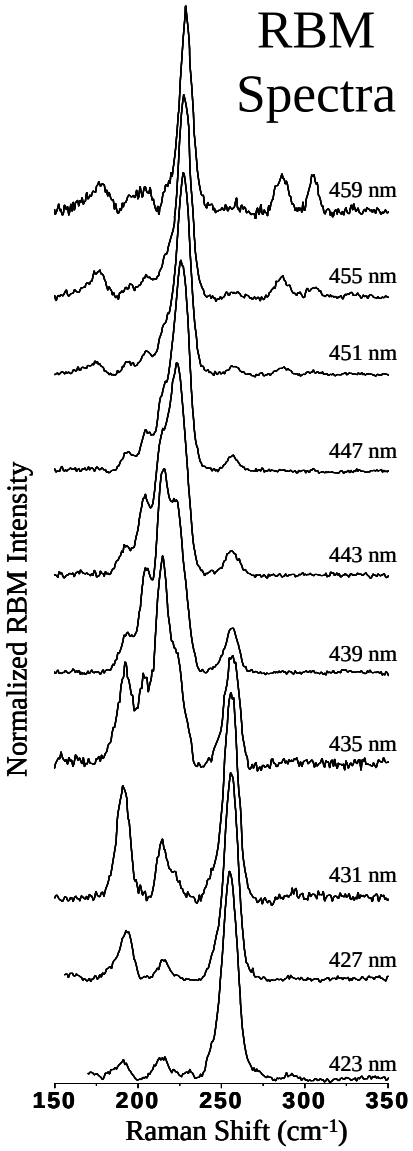

Raman Excitation Map

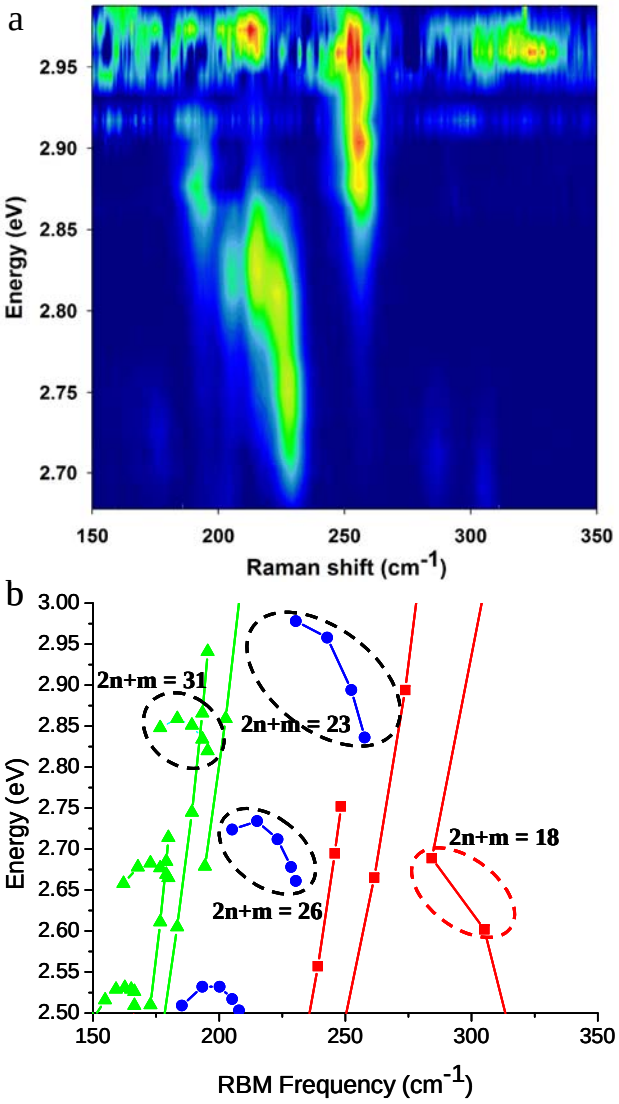

Photoluminescence Excitation Map

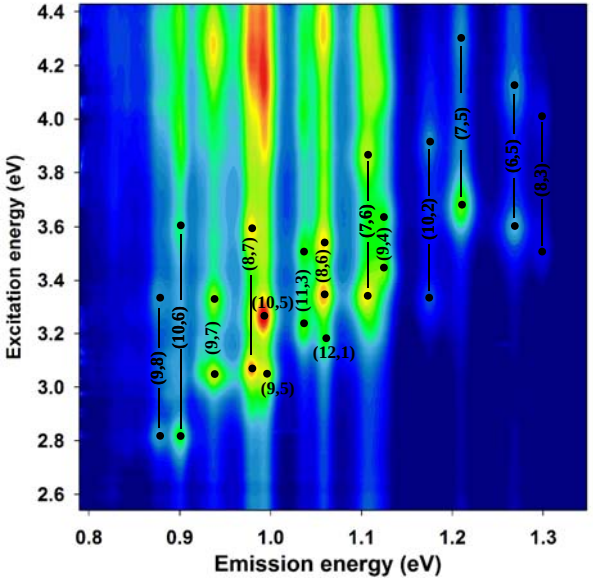

E_{33} (expt.) > E_{33} (ETB)
(For PLE and Raman)

E_{44} trend less clear.

Haroz, et. al., *Phys. Rev. B*, **77**, 125405 (2008).

NASA

Los Alamos

Scaling Law Analysis on Small Diameter Nanotubes

Haroz, et. al., *Phys. Rev. B*, **77**, 125405 (2008).

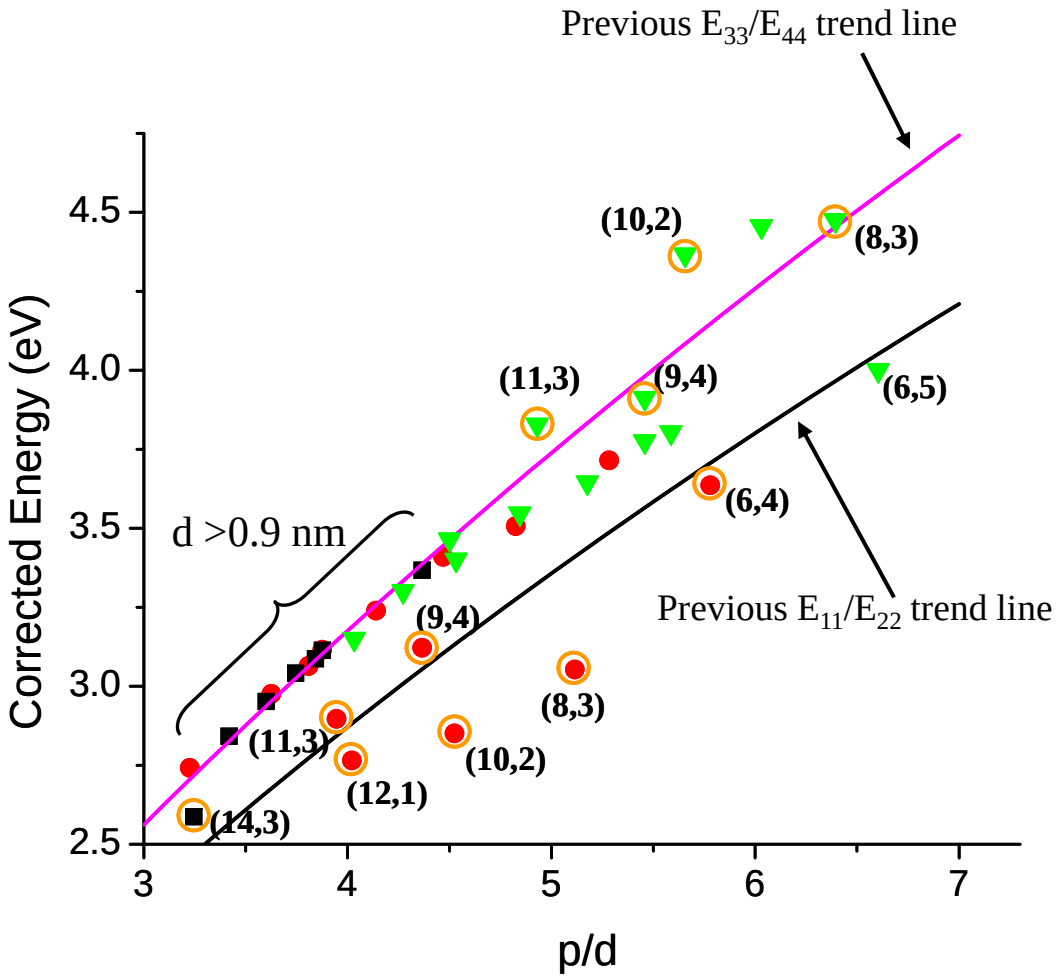

--Large d (>0.9 nm) nanotubes fit well to previous scaling trend.

--Small diameters appear to deviate.

--Significant scatter for selected chiralities.

NASA

Los Alamos

Band Crossing in mod-2 Chiralities

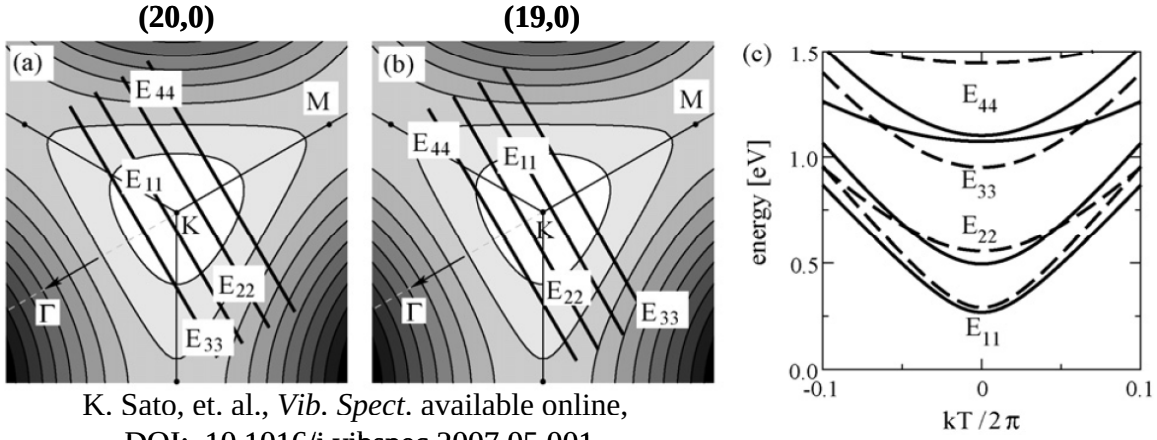

K. Sato, et. al., *Vib. Spect.* available online,
DOI: 10.1016/j.vibspec.2007.05.001

Mod-1 bends away.

Mod-2 bends toward.

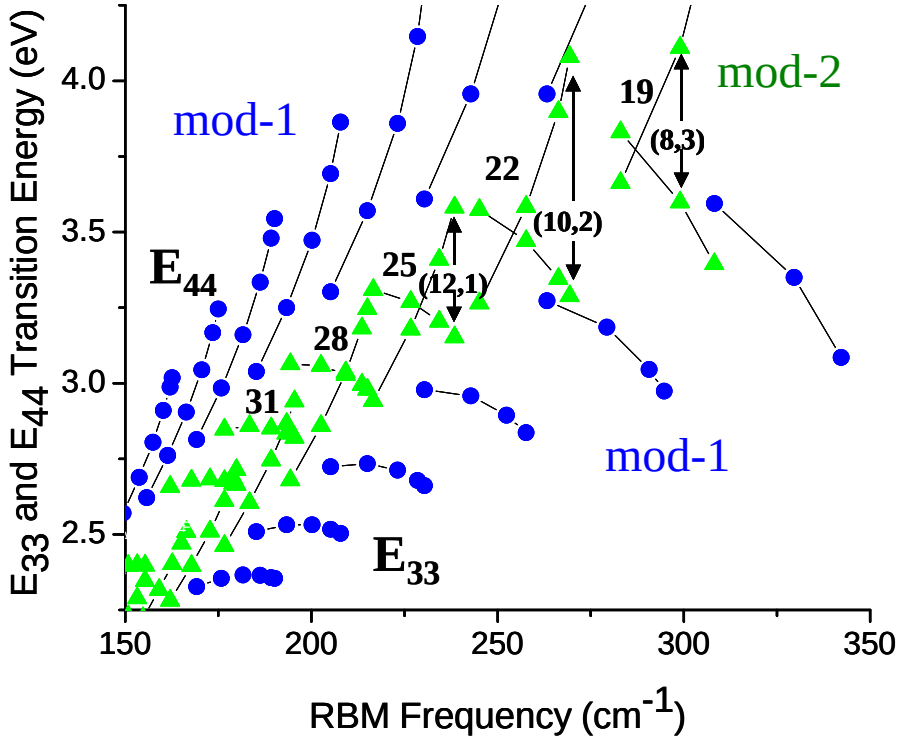

--mod-2 E_{33} transitions cross over E_{44}.

--Transition assignment based on energy ordering does not work.

Chirality Dependence of Many-Body Effects

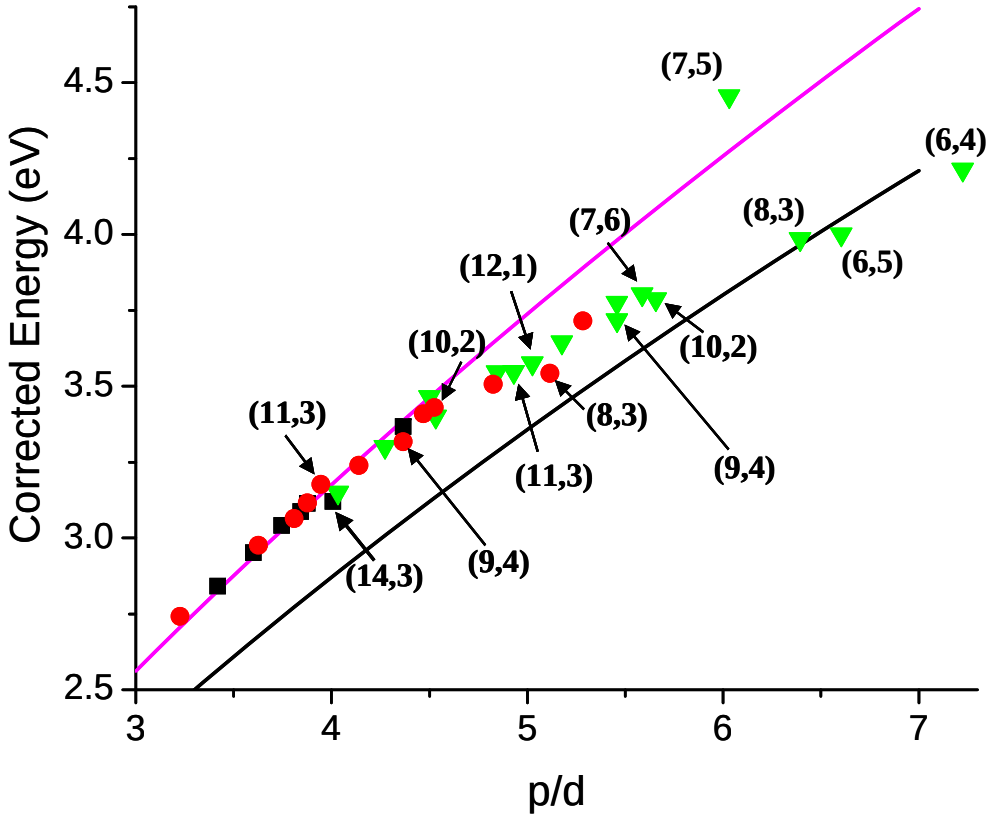

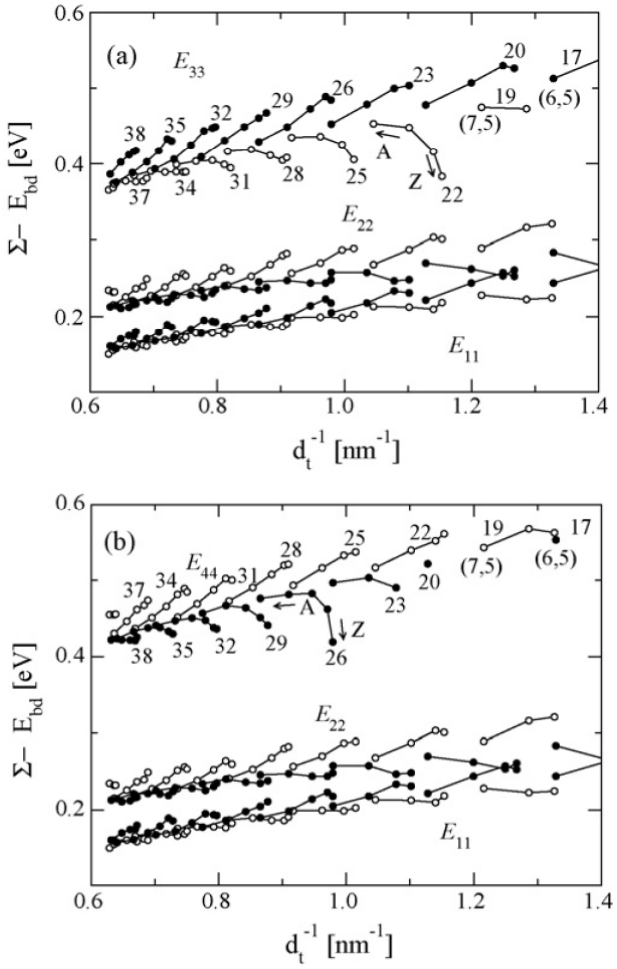

--Downward trend at small d is due to chiral angle dependence of the many-body effects.

--Many-body energy spread in opposite direction from that induced by trigonal warping effects.

K. Sato, et. al., *Vib. Spect.* **45**, 89 (2007)

The (7,5) Assignment

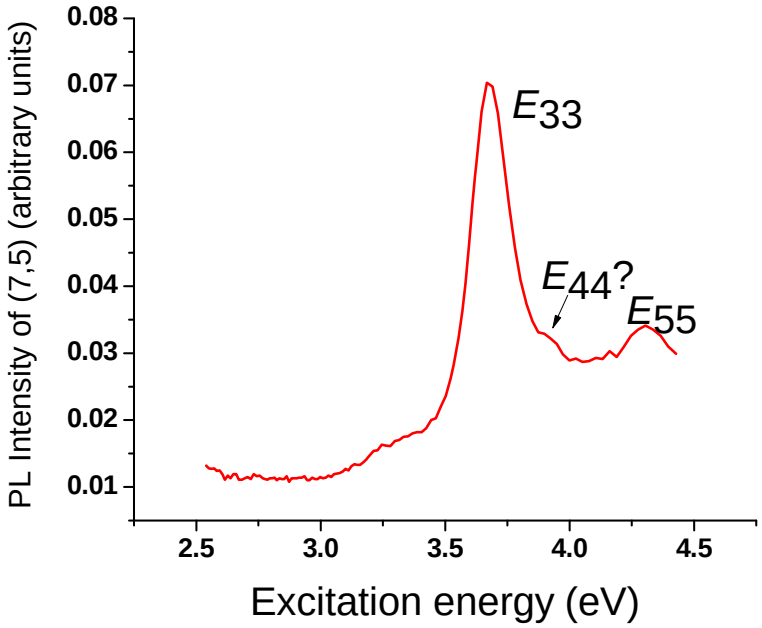

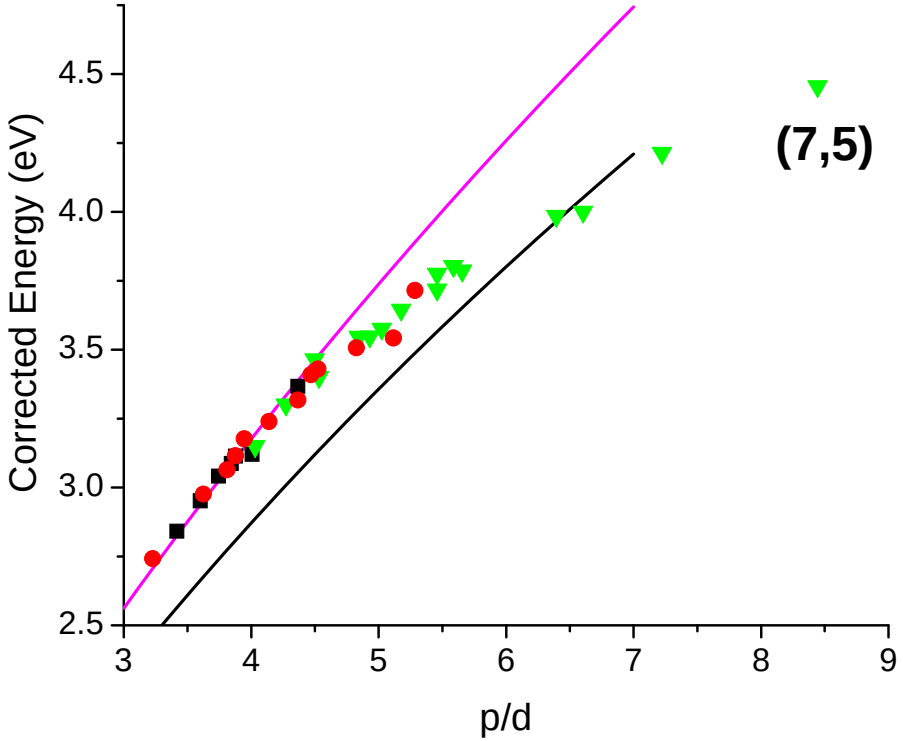

If we consider the (7,5) point as an E_{55} transition energy, it matches the trend with the other chiralities.

Excitons in One-Dimensional Metals

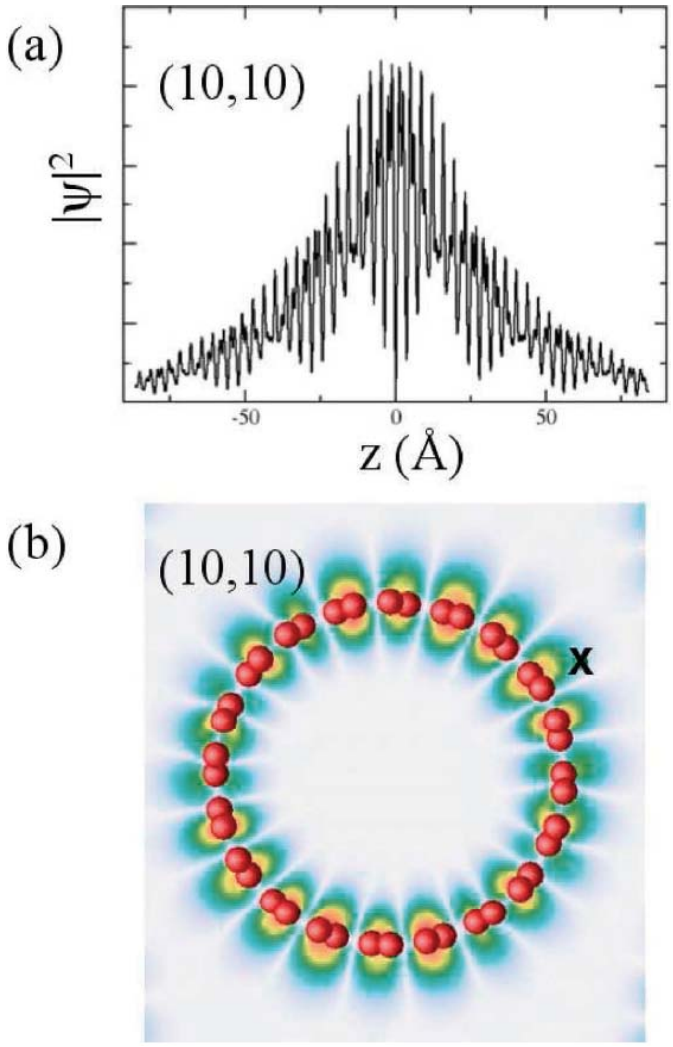

J. Deslippe et. al., *Nano Lett.*, **7**, 1626 (2007).

Strong screening prohibits exciton formation in 2-D and 3-D metals.

Long-range interactions overcome screening in 1-D metallic SWNTs.

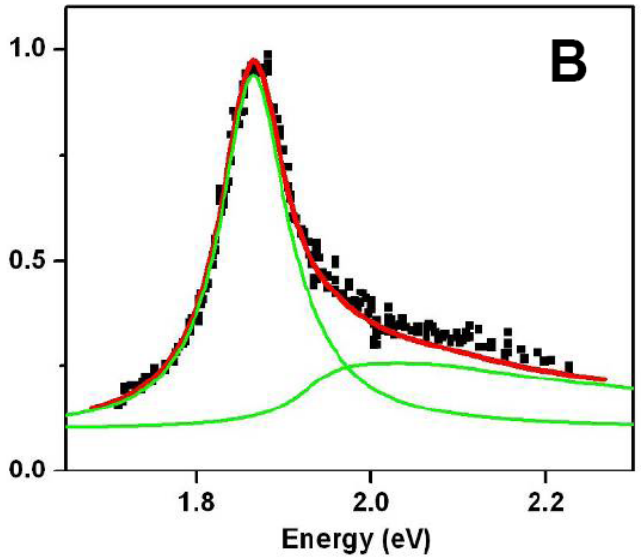

F. Wang et. al., *Phys. Rev. Lett.*, **99**, 227401 (2007).

Raman Analysis of Metallic Nanotubes

S.K. Doorn, et. al., *Phys. Rev. B*, **78**, 165408 (2008)

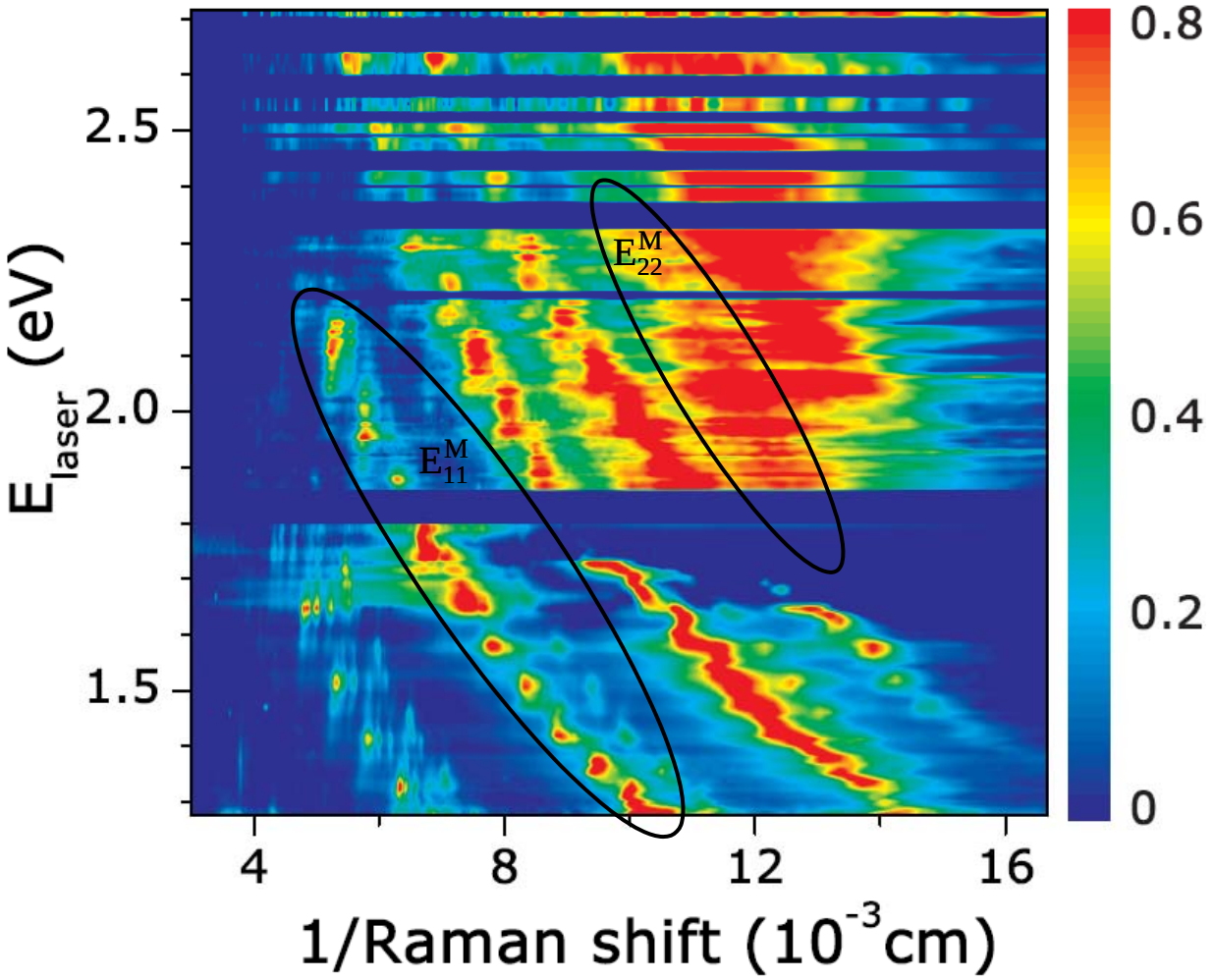

Both E_{11} and E_{22} metallic transitions observed.

Upper branches observed at large diameter.

NASA

Los Alamos

Scaling Analysis of Metallic Energies

S.K. Doorn, et. al., *Phys. Rev. B*, **78**, 165408 (2008)

Semiconducting scaling lines
compared to metallic energy data.

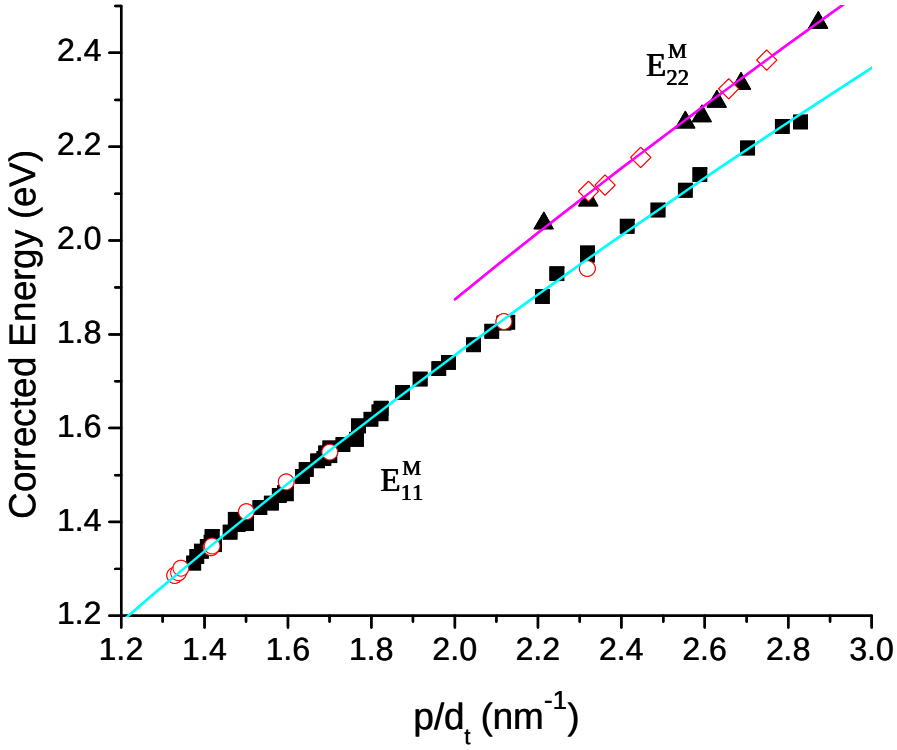

Overlap of metallic scaling with semicond.
consequence of similar sampling of BZ.

Scaling behavior provides indirect
evidence of exciton formation.

NASA

Los Alamos

Schematic Analysis of Relative Scaling Behaviors

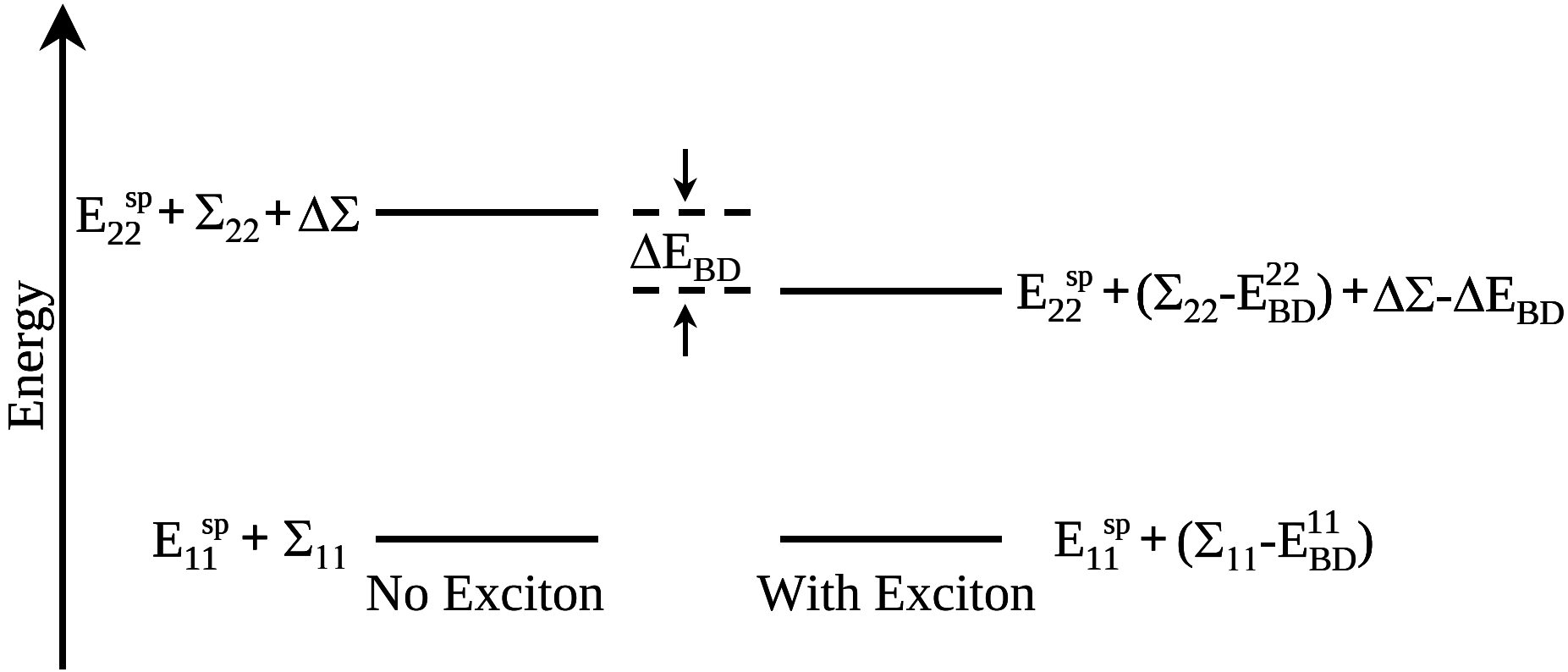

Lack of exciton formation should place E_{22} metallic data above the semiconductor scaling line.

Metallic and Semiconductor Scaling Law Comparisons

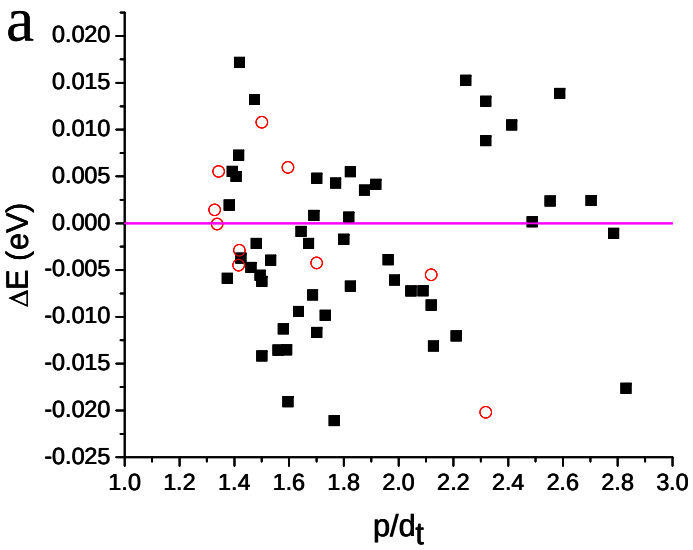

E_{11} metallic data evenly distributed about trend line.

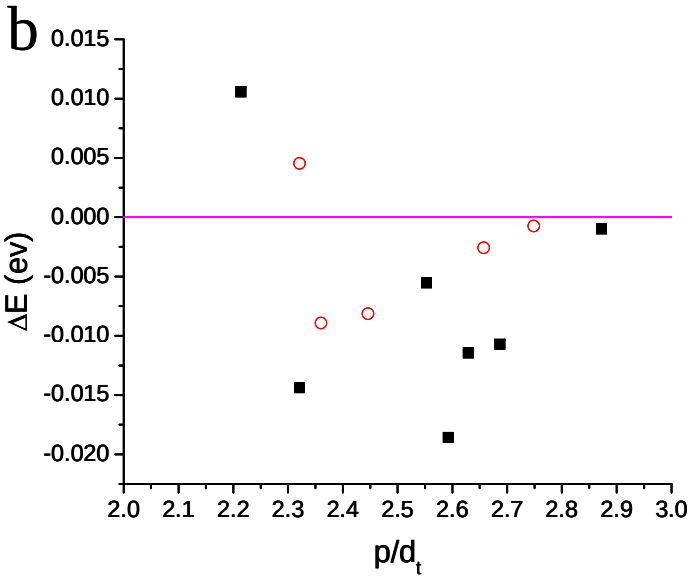

E_{22} metallic data weighted below the trend line.

NNSA

Los Alamos

Exciton-Phonon Coupling In Metallic Nanotubes

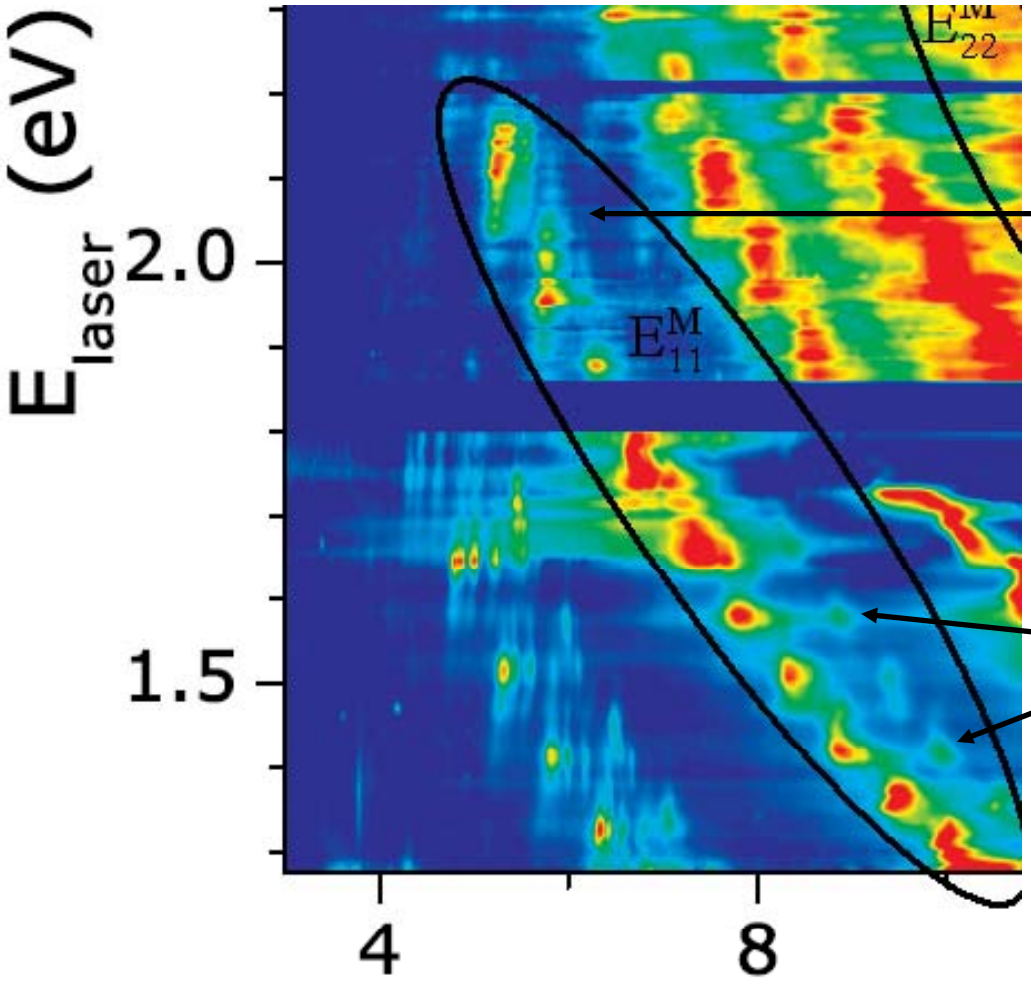

Upper branch features absent at small d. (consequence of coupling)

Upper branch features observed at large d!

NNSA

Los Alamos

Comparable Upper and Lower Branch Intensities

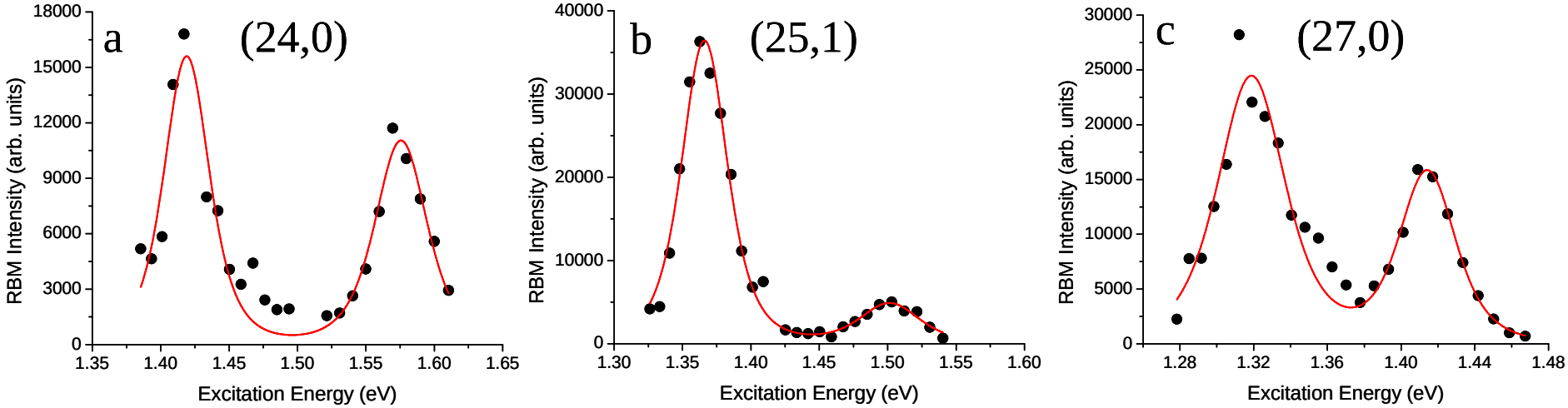

K-Γ vs. K-M Valley Coupling

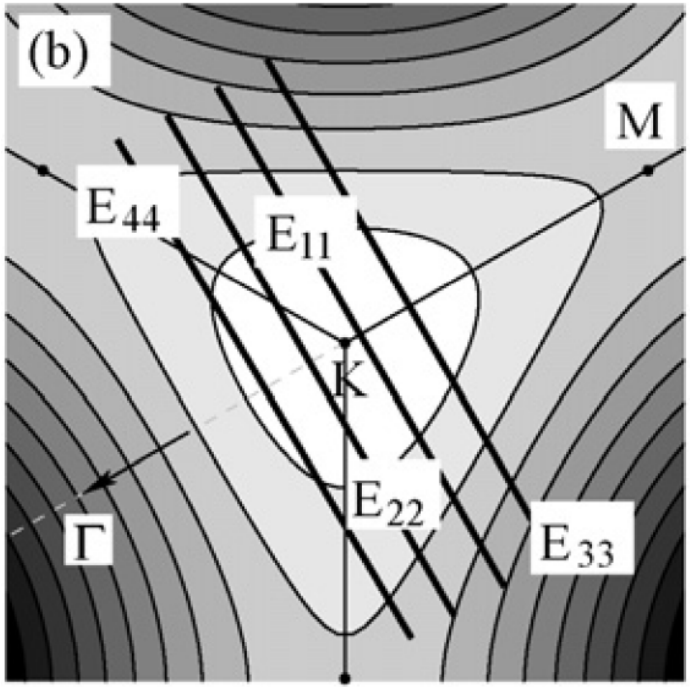

Transitions originating in K-M valley expected to be stronger.

Nodal behavior of coupling.
(E_{11} Excitation)

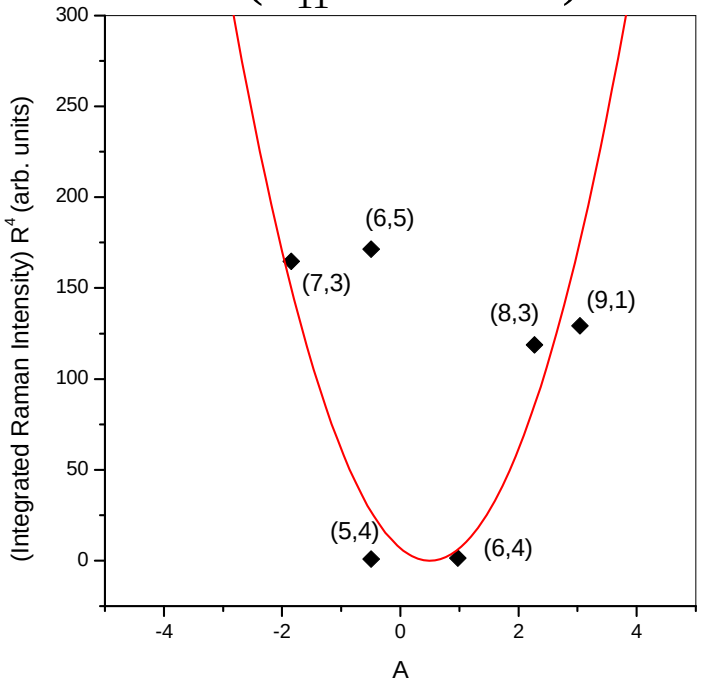

Larger diameter tubes in the K-Γ valley can lie further from the low intensity node.

Goupalov, et. al., *Phys. Rev. B*, **73**, 115401 (2006).

NASA

Los Alamos

General Metallic Intensity Behavior

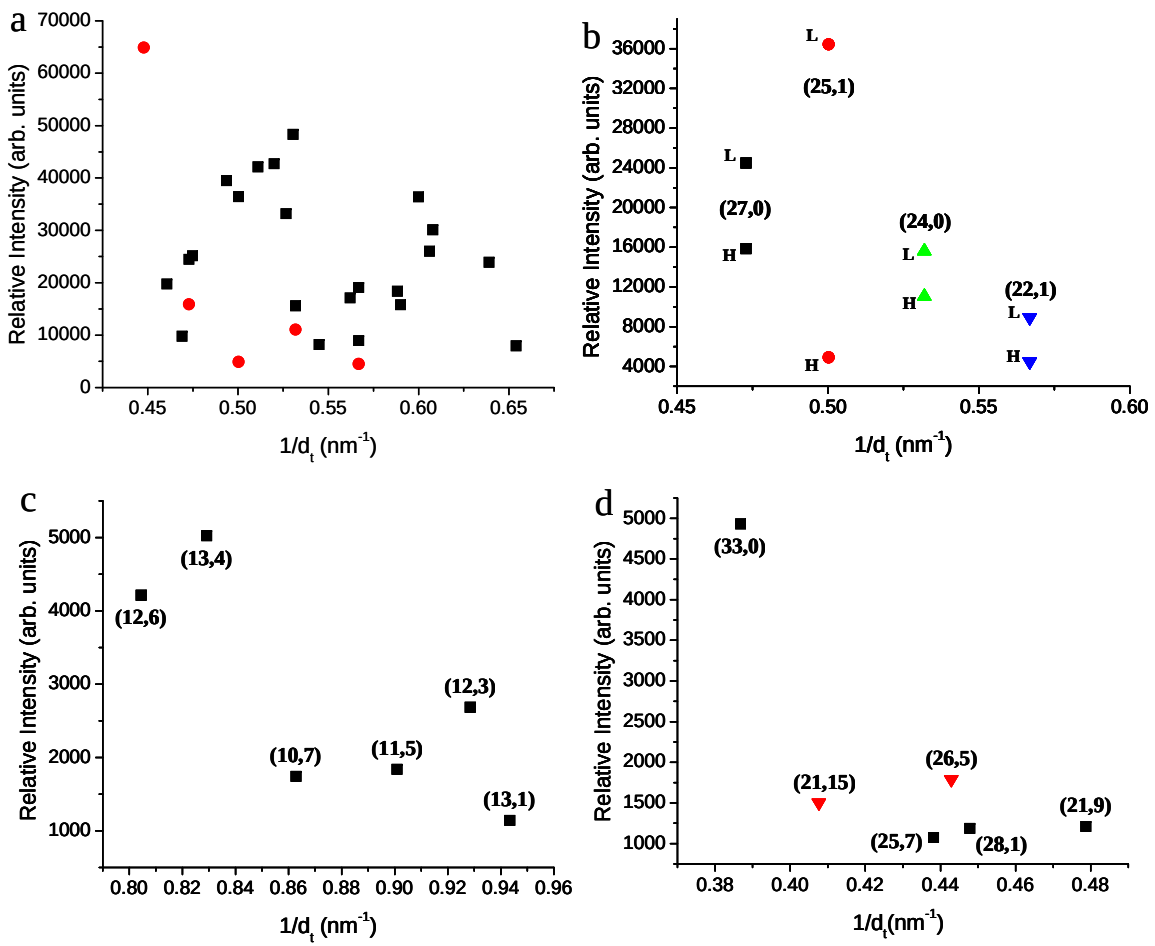

--Intensity decreases as diameter decreases.

--Opposite of expectation based on dependence of exciton-phonon coupling.

NASA

Los Alamos

Diameter Dependence of Gamma

S.K. Doorn, et. al., *Phys. Rev. B*, **78**, 165408 (2008)

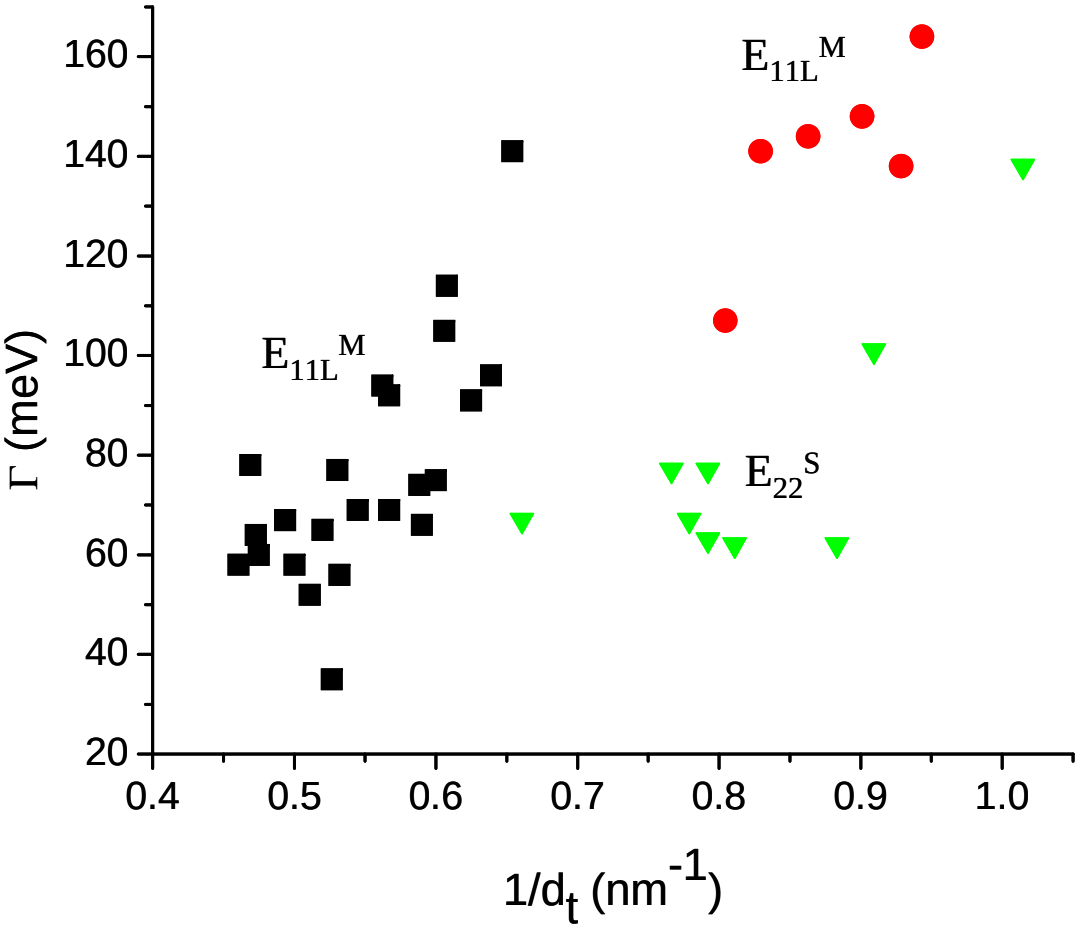

--Γ increases as d decreases.

--Γ influence on intensity overcomes coupling dependence.

--Γ larger for metallics. Consequence of coupling to the plasmon.

NASA

Los Alamos

Expectations From Theory

Park et. al., *Phys. Rev. B*, **74**, 165414 (2006).

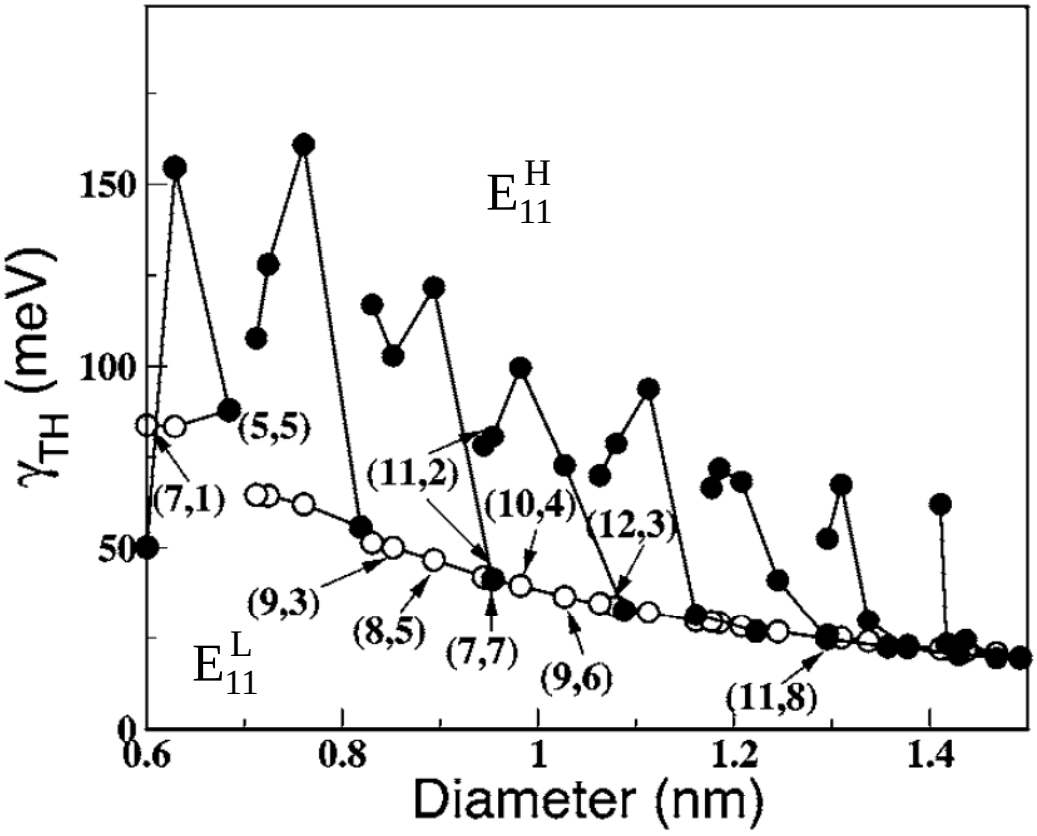

--at large d, Γ increases nearly linearly as d decreases.

--upper and lower branch Γ similar at large d.

Parallels to Semiconductor Intensity Behavior

E11/E22

(n,m)	I_{11}	I_{22}
(6,4)	0.26	0.054
(8,3)	12.6	1.03
(9,1)	15.6	0.33
(5,4)	0.21	0.0037
(6,5)	20.7	0.0720
(7,3)	16.4	0.0014

B.C. Satishkumar, et. al., *Phys. Rev. B*, **74**, 155409 (2006).

E33

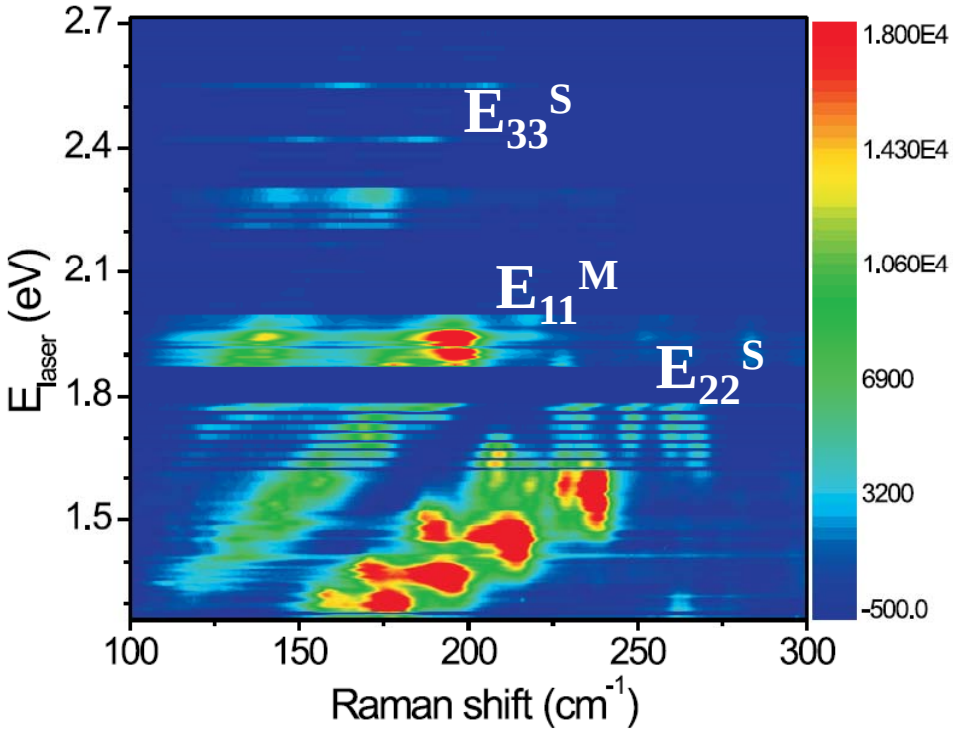

P.T. Araujo, et. al., *Phys. Rev. Lett.*, **98**, 067401 (2007).

E11/E22 profiles and Gammas

$$\alpha = \sum_{i,j} \frac{M_{ee}^{g,i} M_{ee}^{i,g} M_{ep}^{i,j}}{(E_{laser} - E - i\Gamma_r)(E_S - E - i\Gamma_r)}$$

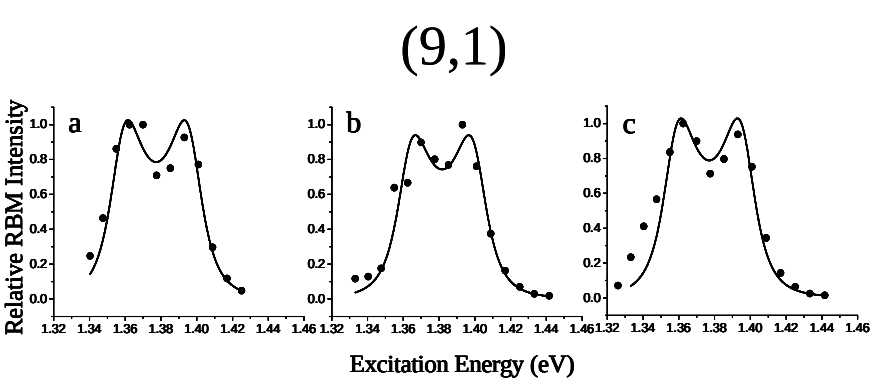

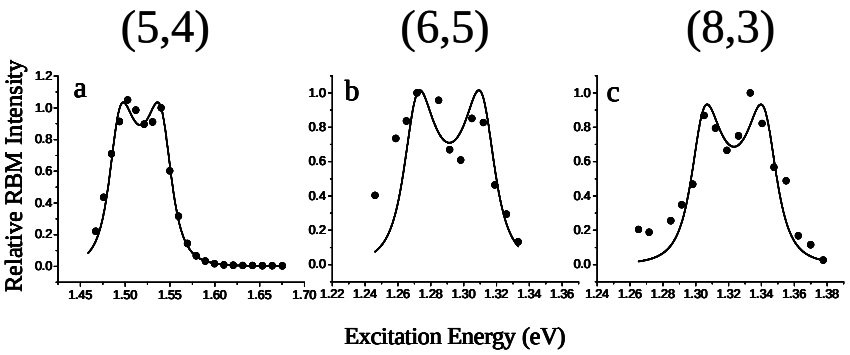

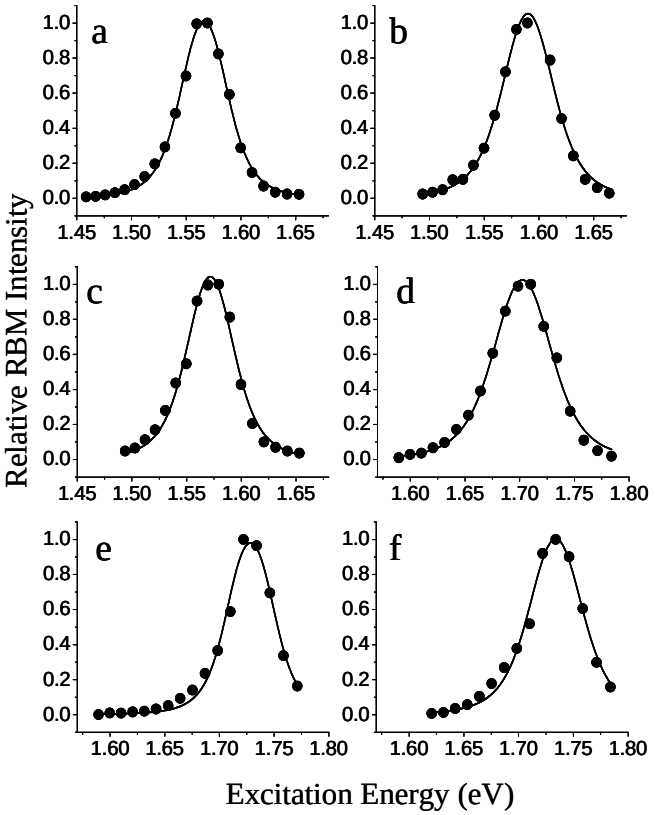

Γ_{11} ~ 20-30 meV

Γ_{22} ~ 60-70 meV

B.C. Satishkumar, S.V. Goupalov, E.H. Haroz, S.K. Doorn, *Phys. Rev. B*, **74**, 155409 (2006).

E33 Excitation Profiles

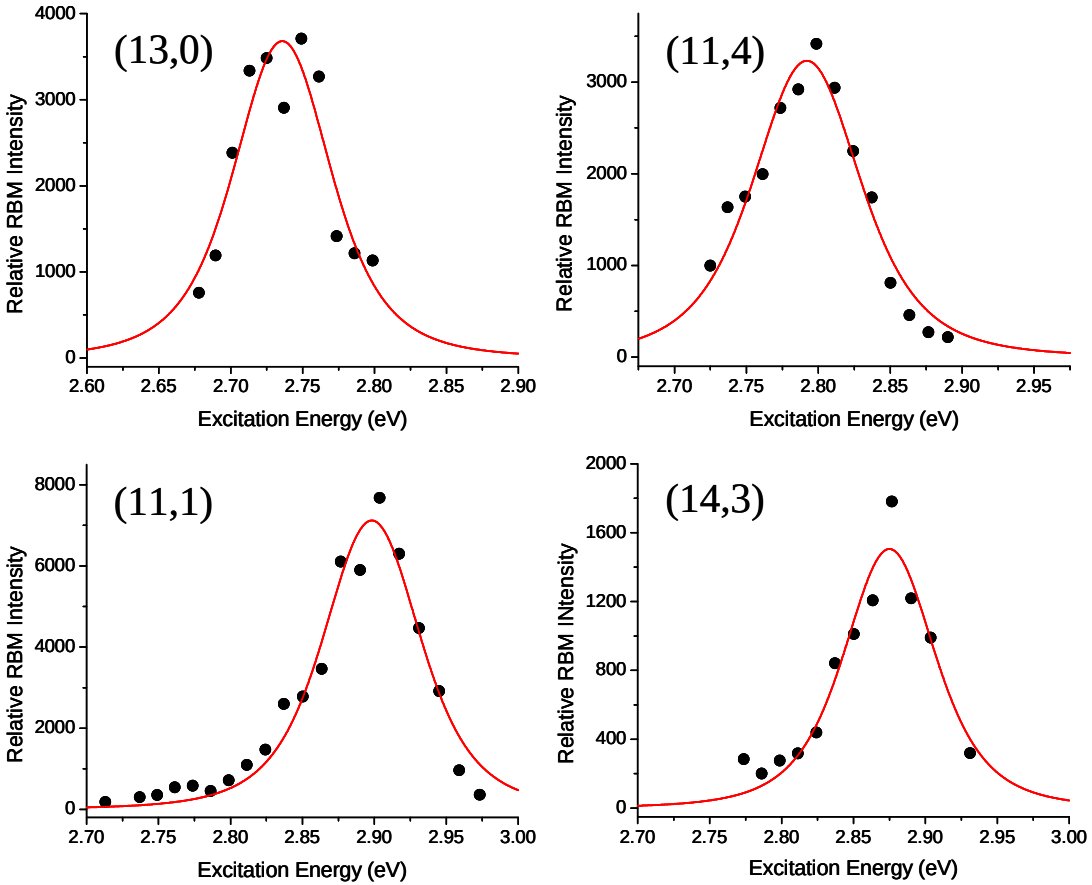

- Trend to larger Γ_{ii} continues.
- Expect D.O.S. and relaxation pathways to increase.
- Agrees with quantum chemical results—increased number of closely spaced states.

Haroz, et. al., *Phys. Rev. B*, **77**, 125405 (2008).

Γ_{33} ~ 110-130 meV

NASA

Los Alamos

Phonon Coupling to Low-Energy Excitations: G-Band

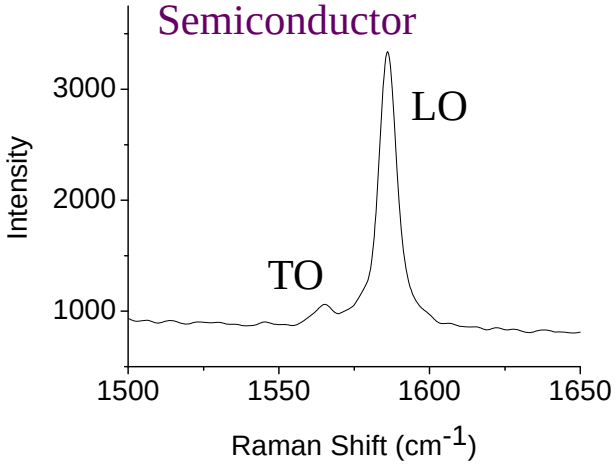

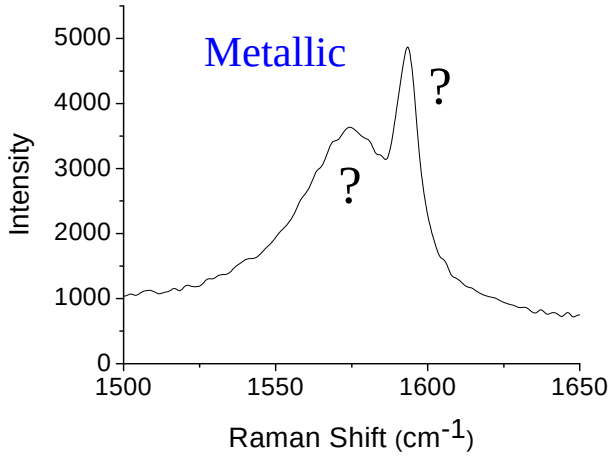

Plasmon Coupling?
-OR-
Excitations at Fermi Level?

Kohn Anomaly

ω decrease for strongly coupled modes

LO: EPC Large
TO: EPC = 0

$$\omega_{LO}^2 = A^2 - B/d; \quad \omega_{TO}^2 = C$$

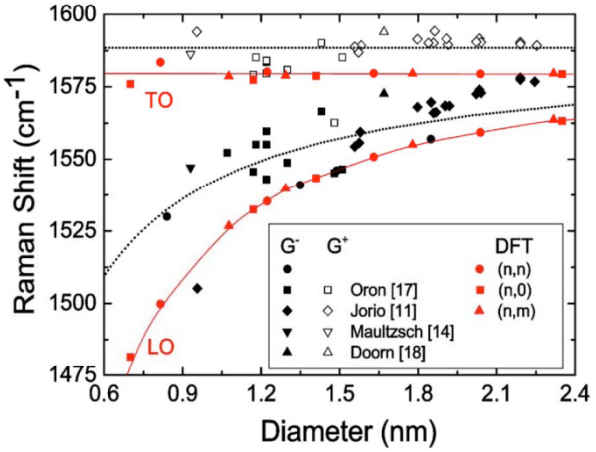

$$\gamma_{\Gamma\text{-LO}}^{EP} = \frac{2\sqrt{3}\hbar a_0^2}{\pi M \omega_\Gamma \beta}\frac{\langle D_\Gamma^2\rangle_F}{d}; \quad \gamma_{\Gamma\text{-TO}}^{EP} = 0$$

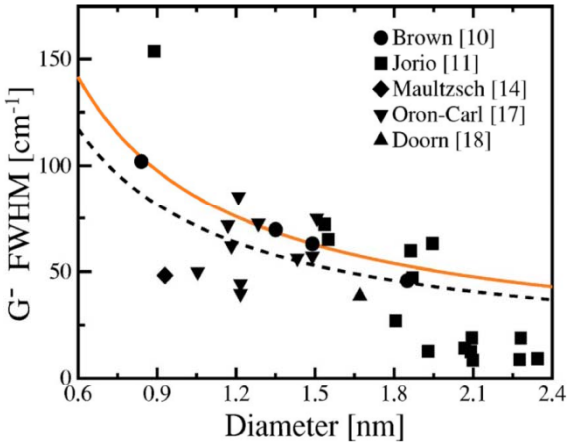

Lazzeri, et. al., *Phys. Rev. B*, **73**, 155426 (2006).

G-Band Lineshape: Gating and Chirality Effects

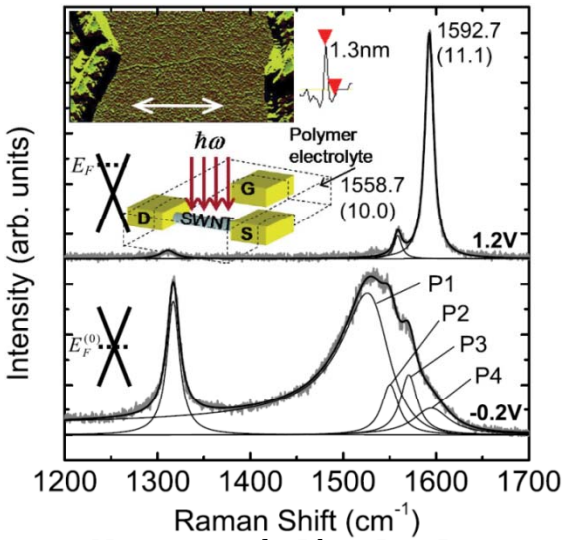

Nguyen, et. al., *Phys. Rev. Lett.* **98**, 145504 (2007).

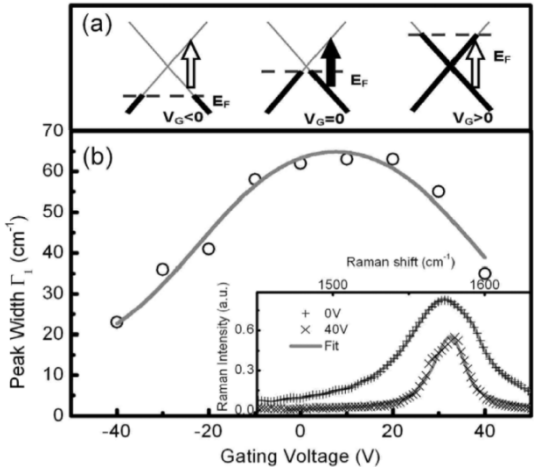

Wu, et. al., *Phys. Rev. Lett.* **99**, 027402 (2007).

Electrostatic Gating

--Shifts Fermi Level

--Excitations > 200 meV
no G-band coupling

--LO Narrows

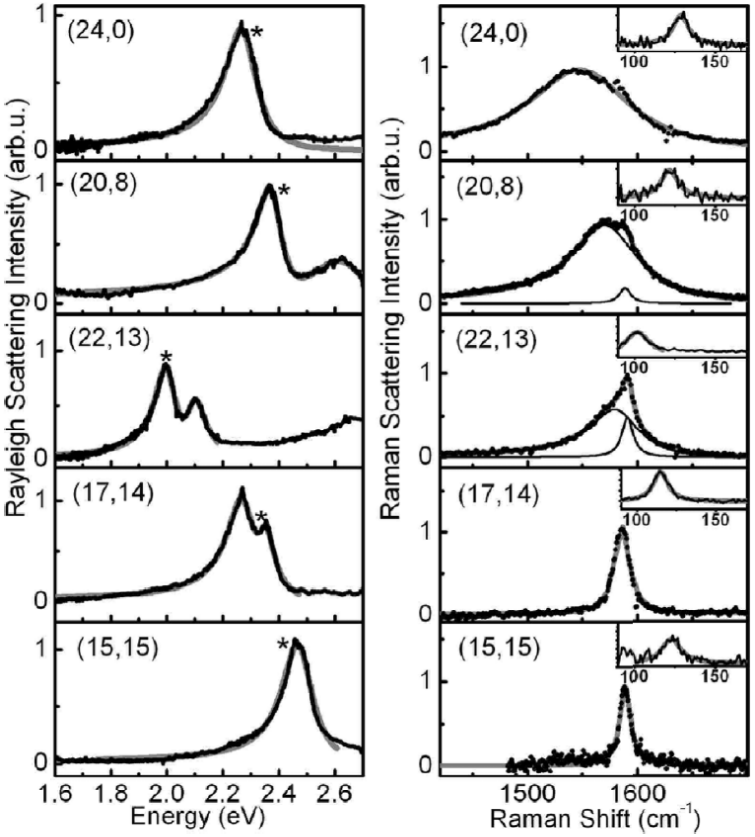

Wu, et. al., *Phys. Rev. Lett.* **99**, 027402 (2007).

Lineshape inherent to single metallic tube.

Strong chirality dependence.

Is single sharp G^+ band a general result for armchairs?

NASA

Los Alamos

Ensemble Spectra: Approaching the Pure Armchair Limit

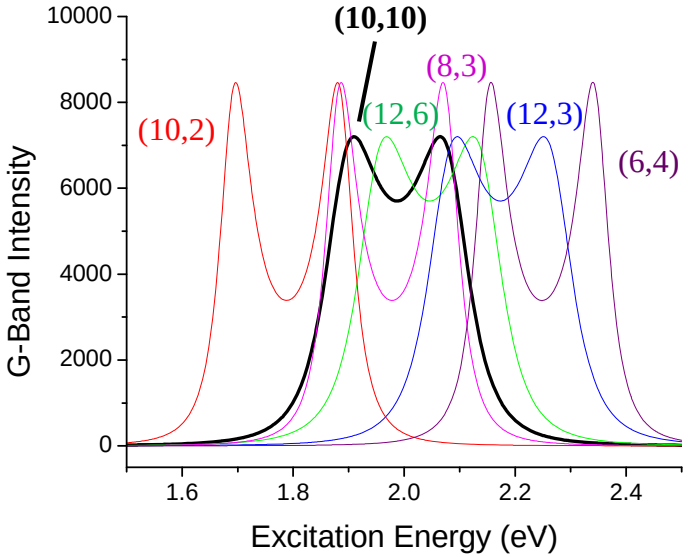

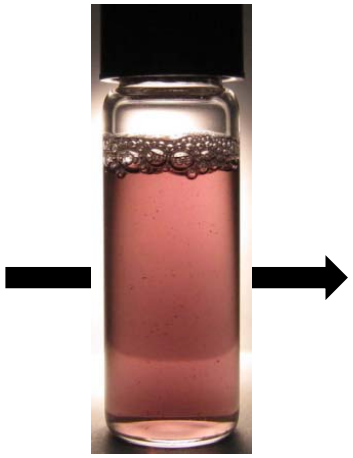

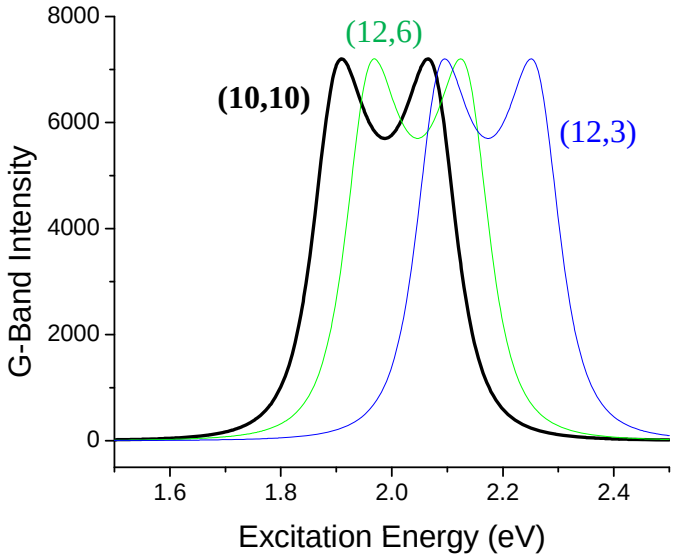

G-Band not as Clean as RBM

?

DGU Separations: "Eliminate" Semiconductors

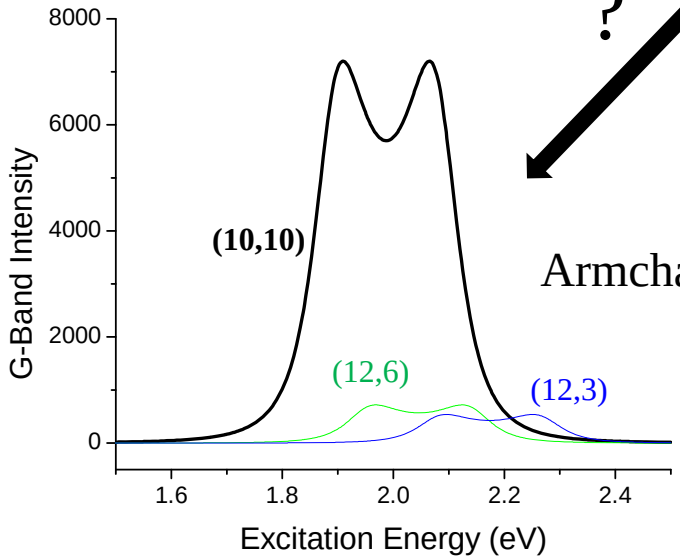

Armchair Enrichment?

NASA

Los Alamos

Density Gradient Separations

- Widely used in biochemistry and pharmaceutical industry.
- Separation based on very subtle differences in buoyant densities of components—diameter dependent.
- Ultracentrifugation within a preformed gradient that varies in density with height.
- Nanotubes separate into levels of gradient of matching density upon ultracentrifugation.
- Typically requires use of cosurfactant (various combinations of SDS, SDBS, cholates) suspension of nanotubes.

Summary

Raman is a sensitive probe of structure,
phonon-coupling, and nature of excited states.

First evidence for transition cross-over effect
and chirality dependence of many-body influences.

Support for the existence of excitons in 1-D metals.

First Raman evidence of metallic upper branches.

G+ (TO) dominance in armchair spectra is a general behavior.

Acknowledgements

Curvature Effects On E33/E44
Erik Haroz (Rice)
Sergei M. Bachilo (Rice)
R. Bruce Weisman (Rice)

E_{33}/E_{44} and Metallics
Ado Jorio (Belo Horizonte)
Paulo Araujo (Belo Horizonte)
Shigeo Maruyama (Univ. of Tokyo)
Kenji Hata (AIST)

Armchair Raman
Erik Haroz (Rice)
Jun Kono (Rice)